

Sampling Strategies for Robust MLIPs

Dr. Michael J. Waters

michael.j.waters@northwestern.edu

Prof. James M. Rondinelli

jrondinelli@northwestern.edu

AIMS 2024

2024-07-18

Session IV



Grant No. N00014-20-1-2368

Northwestern



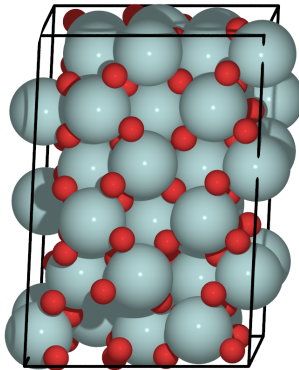
Overview

1. Introduction to sampling strategies
2. Evolving structures without MD
3. Evolving structures and (hyper)active learning
4. Active barrier learning

Spectrum of Disorder for Structure Synthesis

Known Structures

- Selected using a priori knowledge

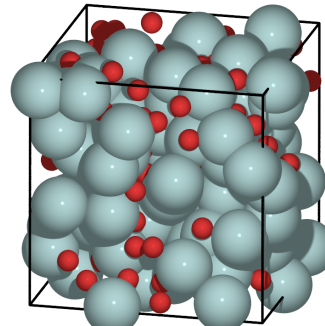


Decreasing a priori knowledge

Simulation cell related to lattice parameter

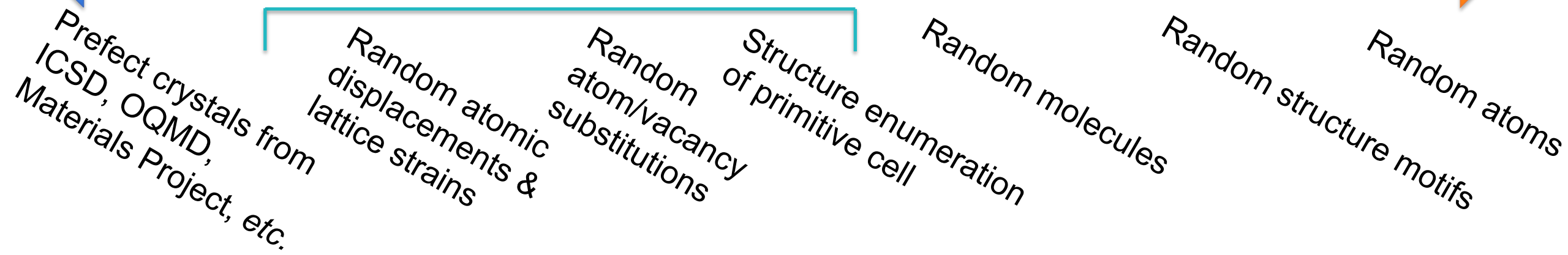
Randomized Structures

- Constructed by randomly inserting subcomponents



Simulation cell informed by interaction ranges only

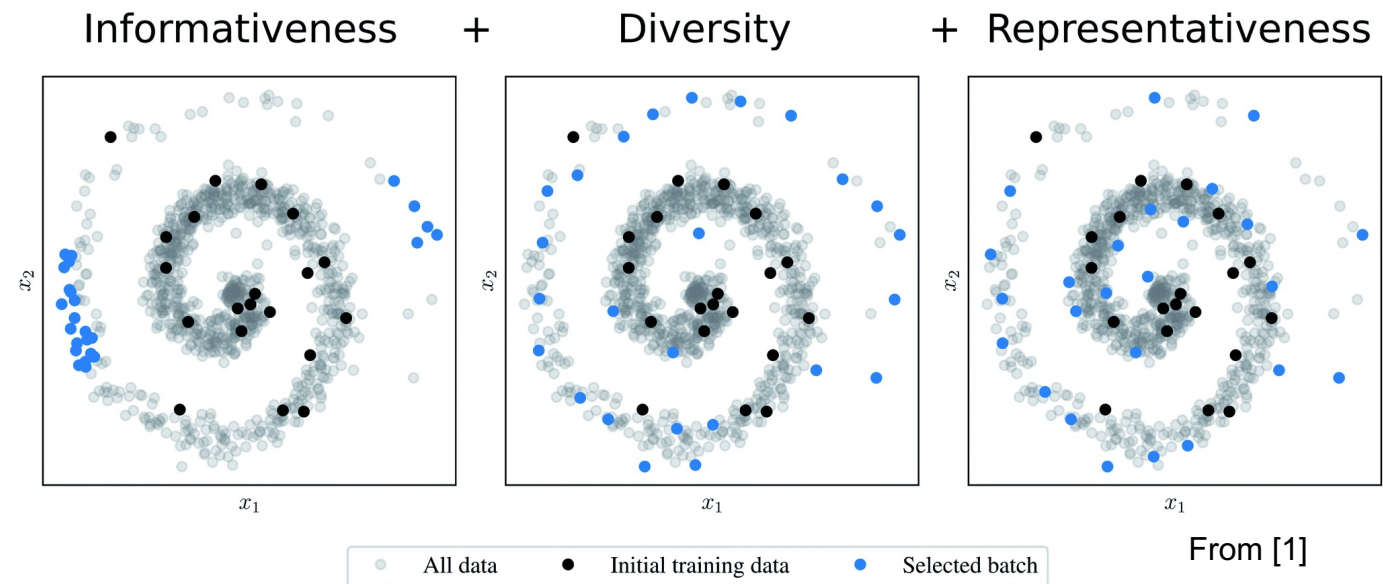
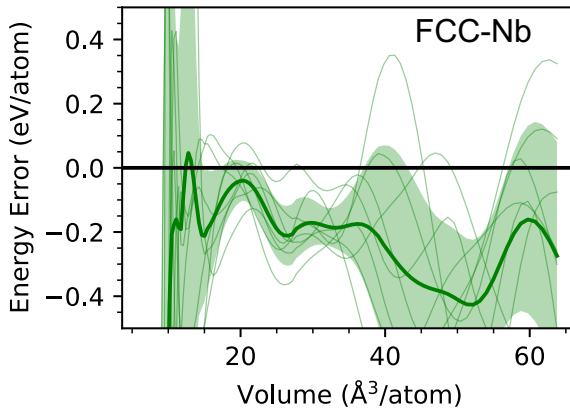
Derived Structures



Structure Sampling Strategies

Feature space

- Select training data to tune feature space distribution
- Independent of model parameterization



From [1]

Model inference

- Select training data based on current model outputs
- Ex. on-the-fly active learning → evolving structure and selecting high uncertainty structures from trajectory

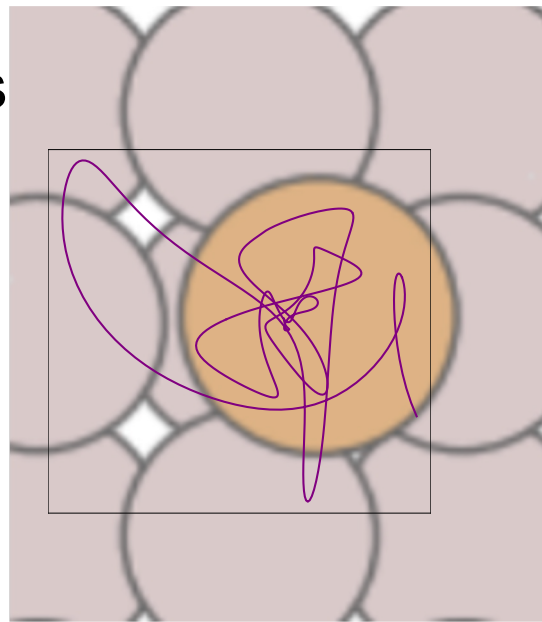
Regardless of strategy, an initial dataset is required → Why not some (AI)MD?

Evolving structures without MD

Sampling MD trajectories for training data

MD Pros

- Autonomous → evolves structure without input
- Sequential structure evolution → SCF is more stable/faster for AIMD
- Generally available



Cu adatom MD trajectory

MD Cons

- Time integration
 - Redundant local sampling
 - Large time steps risks numerical instability
 - PES not a function of time
- Rare events are rare
- NVT: PES not a function of temperature
- NVE: difficult to control E in practice...

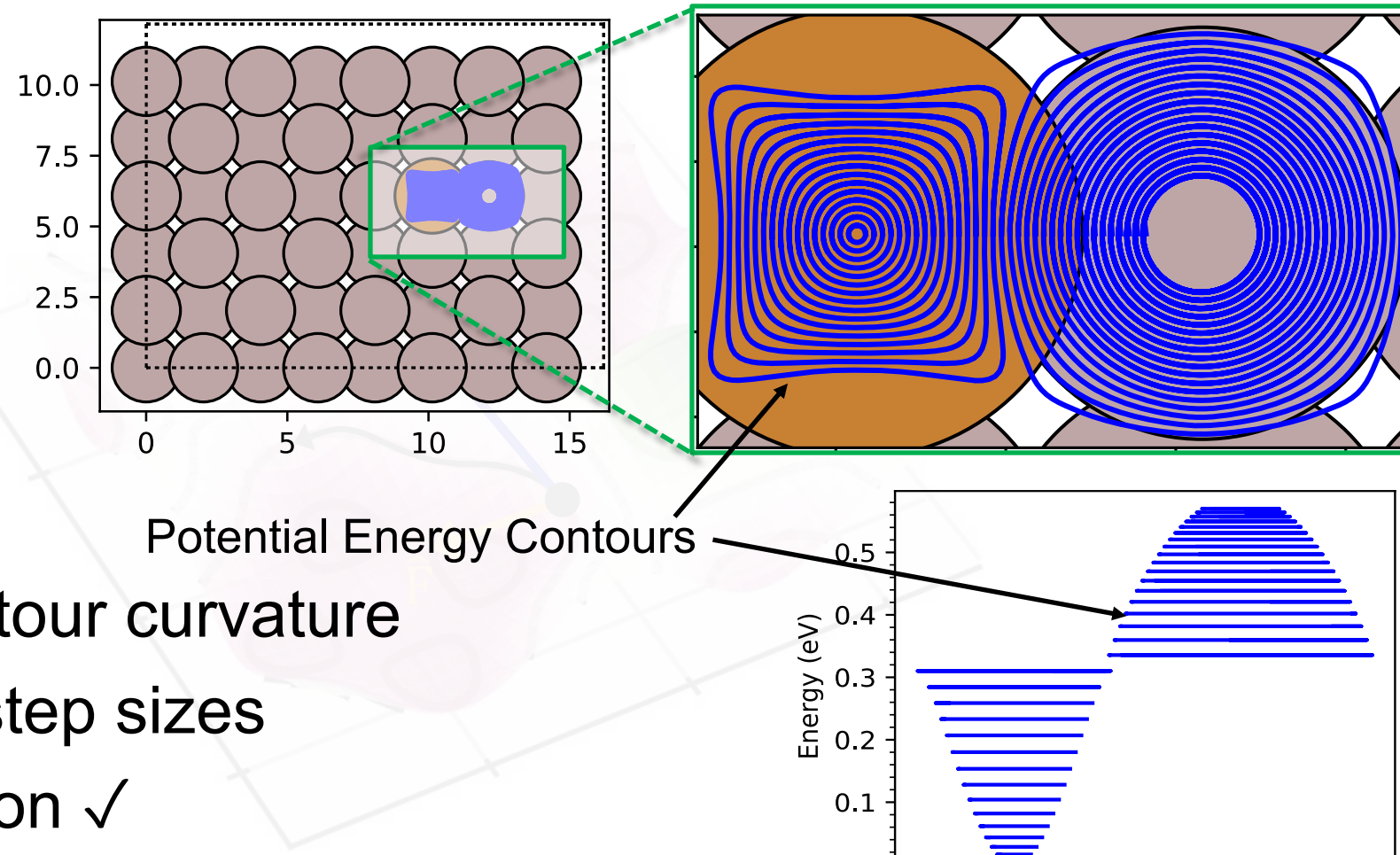
Solutions

- Use active learning/sample dropout to reduce redundancy
 - Applicable to any structure evolution method
- Invent new kinematics to take large steps while controlling E



Contour Exploration with Potentiostatic Kinematics¹

- Set the potential energy target
- Move \parallel to **contour tangent**, \hat{T} , and \perp to **forces**, \hat{F}
- Step sizes scaled to contour curvature
 - Permits large stable step sizes
- Has autonomous evolution ✓
- Included in  !²

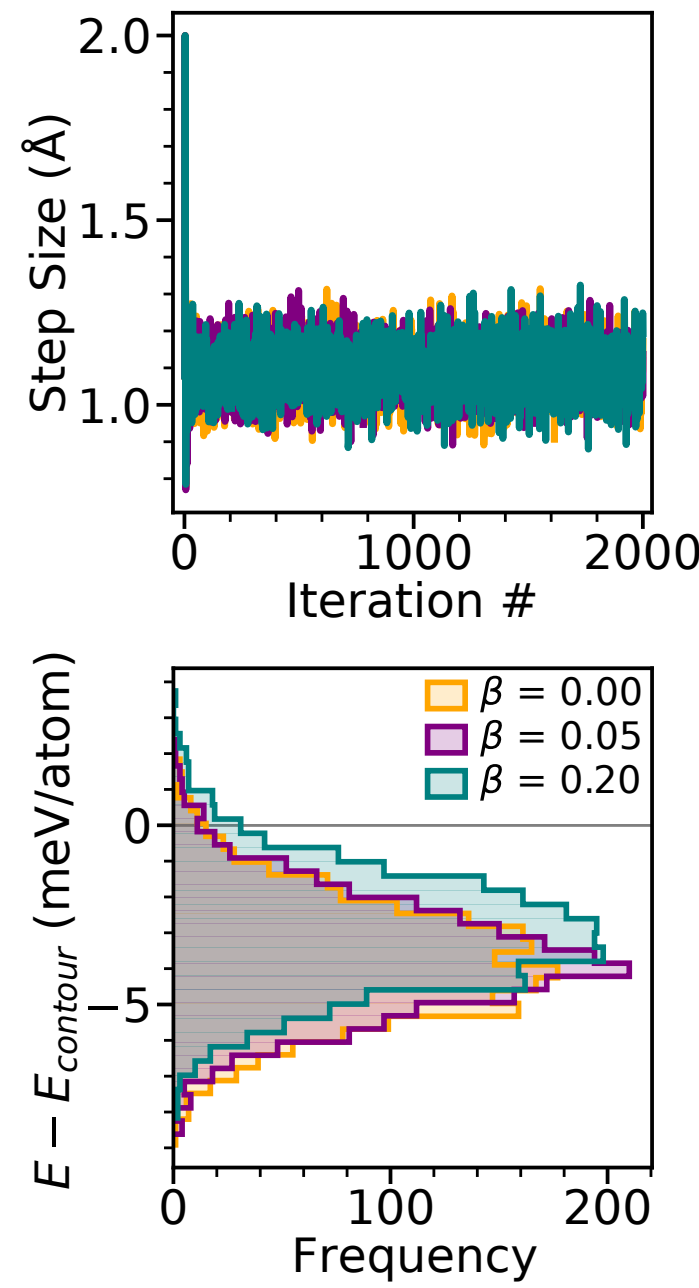
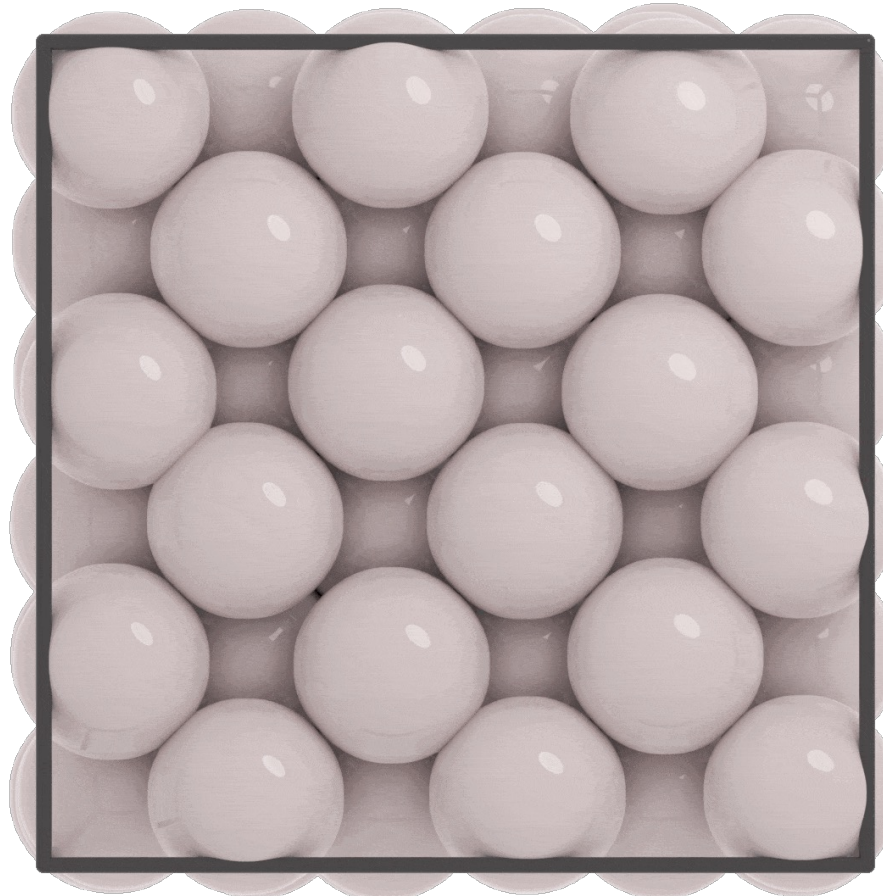


¹Michael J Waters and James M Rondinelli 2021 *J. Phys.: Condens. Matter* **33** 445901 DOI 10.1088/1361-648X/ac1af0

²wiki.fysik.dtu.dk/ase/_modules/ase/md/contour_exploration.html

Contour Exploration in Bulk

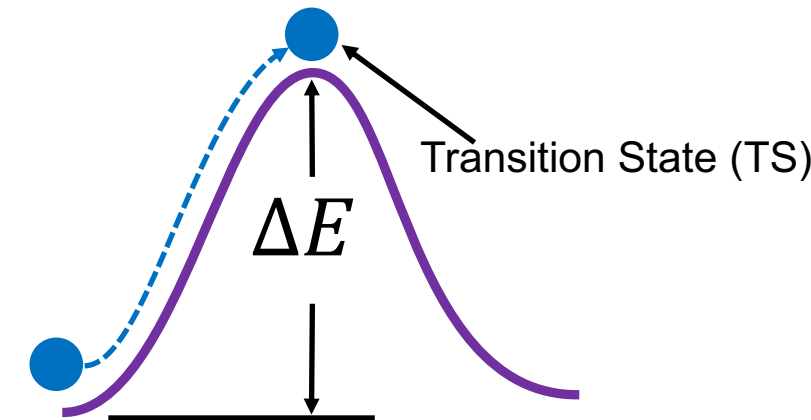
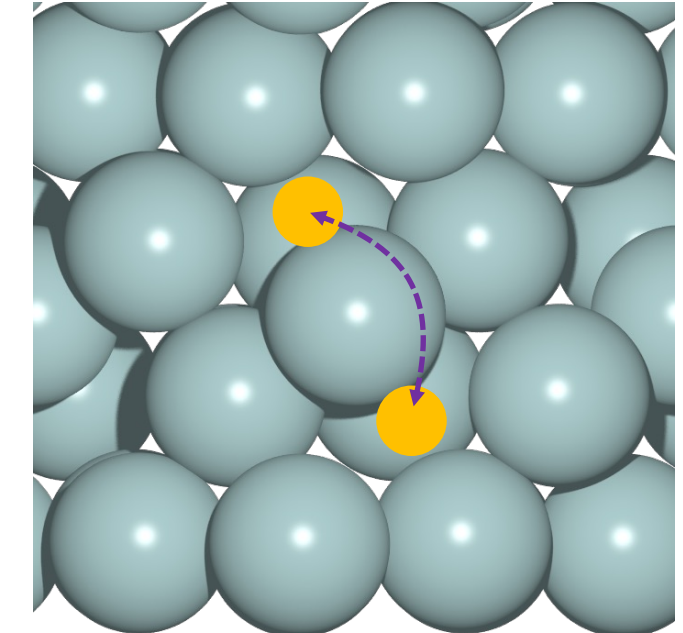
- 3x3x3 FCC Al cell
- Potential energy target: 164 meV/atom
 - 5% of cohesive energy
- EMT potential model



Dimer Method

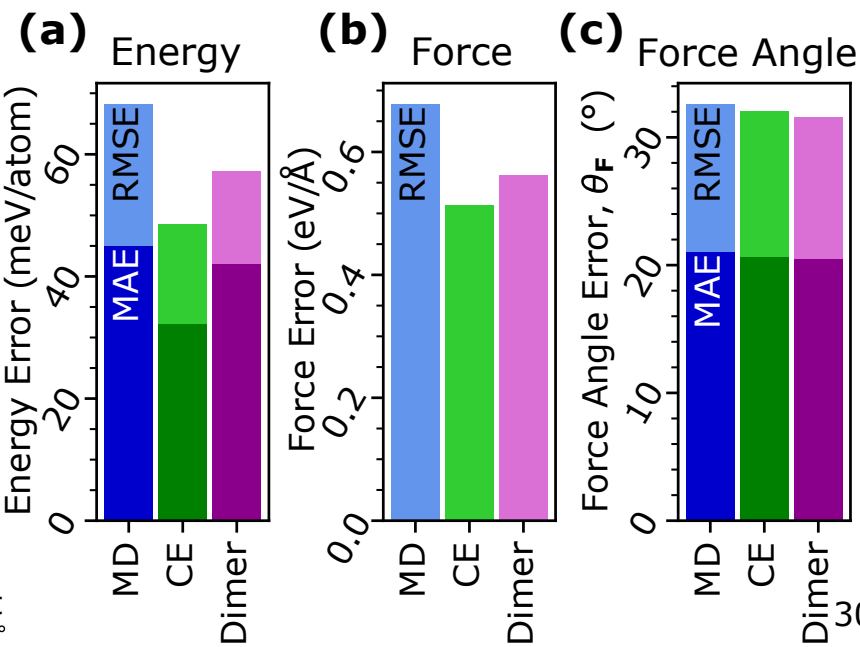
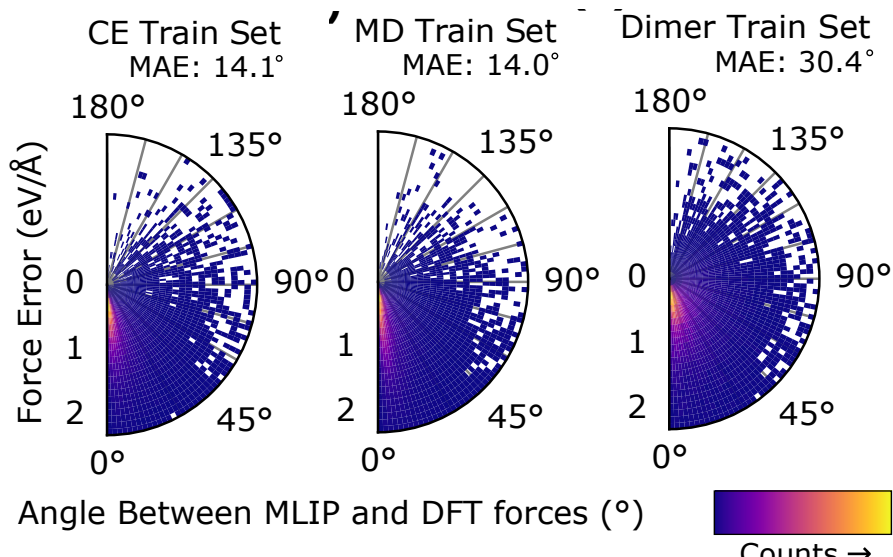
- Evolves towards saddle points *i.e.* reaction barriers/transition states
 - Important rare events
- Not tuned by temperature or time
 - High energy structures can occur during search
- Autonomous evolution ✓

→ Three-way benchmarking time



MD, CE, and Dimer Benchmarking: Accuracy

- Zr/O – random + derived oxide/metal phases
- Only trajectory sampling
 - Unbiased by active learning
- BP-NN trained in AMP
- Test set mix of withheld trajectories from all three

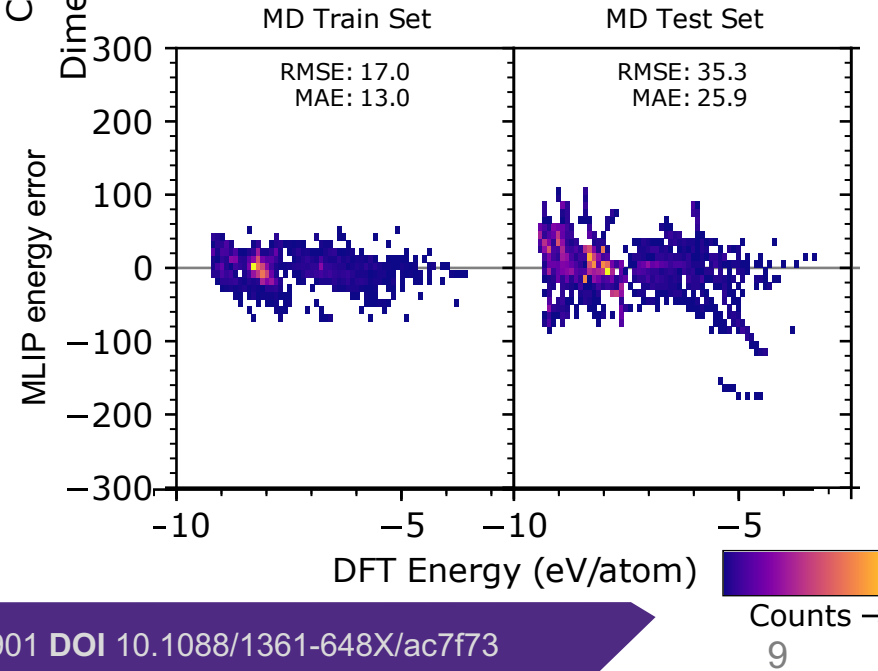


Best Accuracy: CE

MD trajectories can
be seen in error

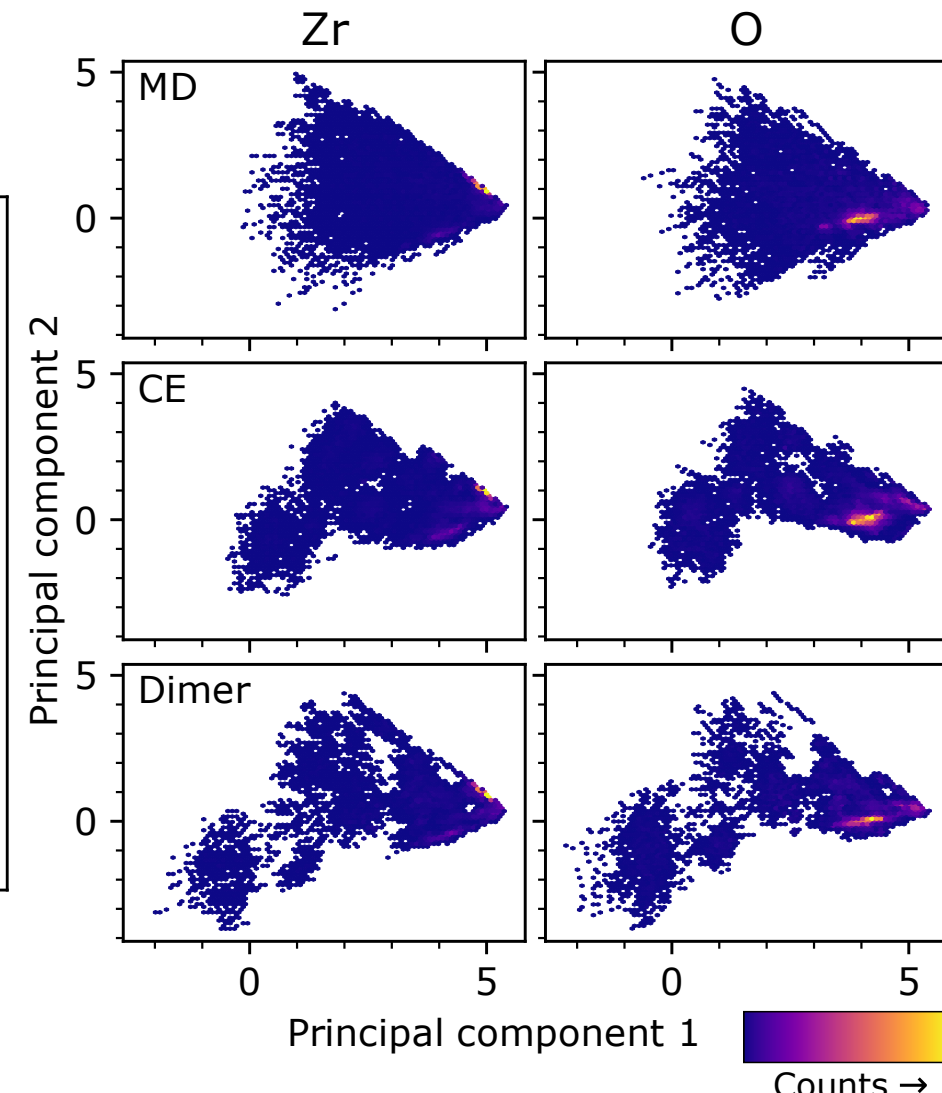
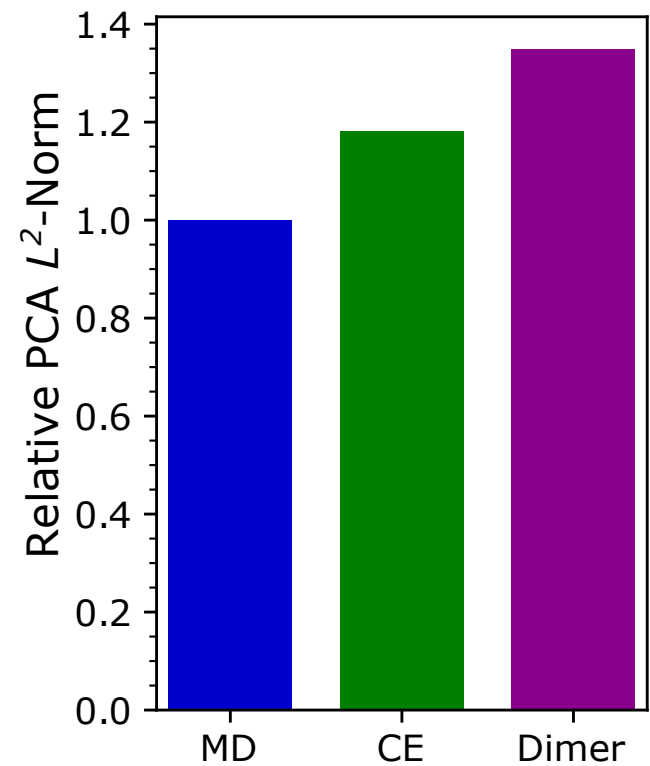
Dimer data has 2x the
angle MAE in train set!

$$\theta_F = \cos^{-1} \left(\frac{\mathbf{F}_{MLIP} \cdot \mathbf{F}_{DFT}}{|\mathbf{F}_{MLIP}| |\mathbf{F}_{DFT}|} \right)$$



MD, CE, and Dimer Benchmarking: Diversity

- BP spatial descriptor PCA
- Dimer: most diverse, hardest to fit data
- CE: Best model performance, easier to tune



Evolving structures and (hyper)active learning

(Hyper)Active Learning

- **Active learning:** picking structures with highest uncertainty
- **Hyperactive learning:** +biasing atomic motion with adversarial attack
 - Typically, with MD¹⁻³
 - Metadynamics⁴
- Easy to implement with committee models¹

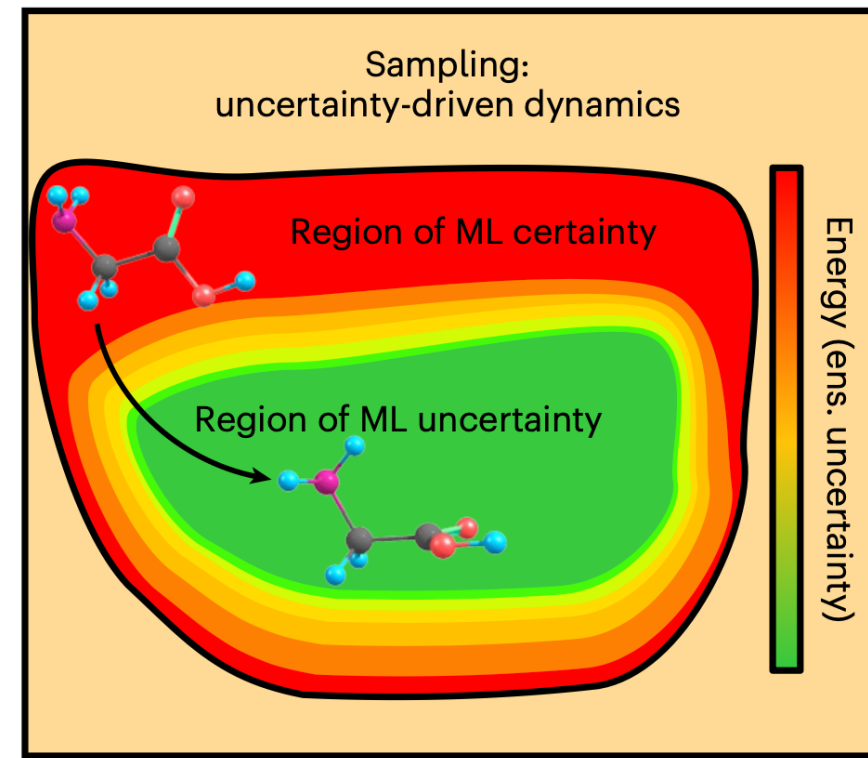


Fig. 1a from [3]

¹Christoph Schran, Krystof Brezina, Ondrej Marsalek; J. Chem. Phys. 14 Sept. 2020; 153 (10): 104105. <https://doi.org/10.1063/5.0016004>

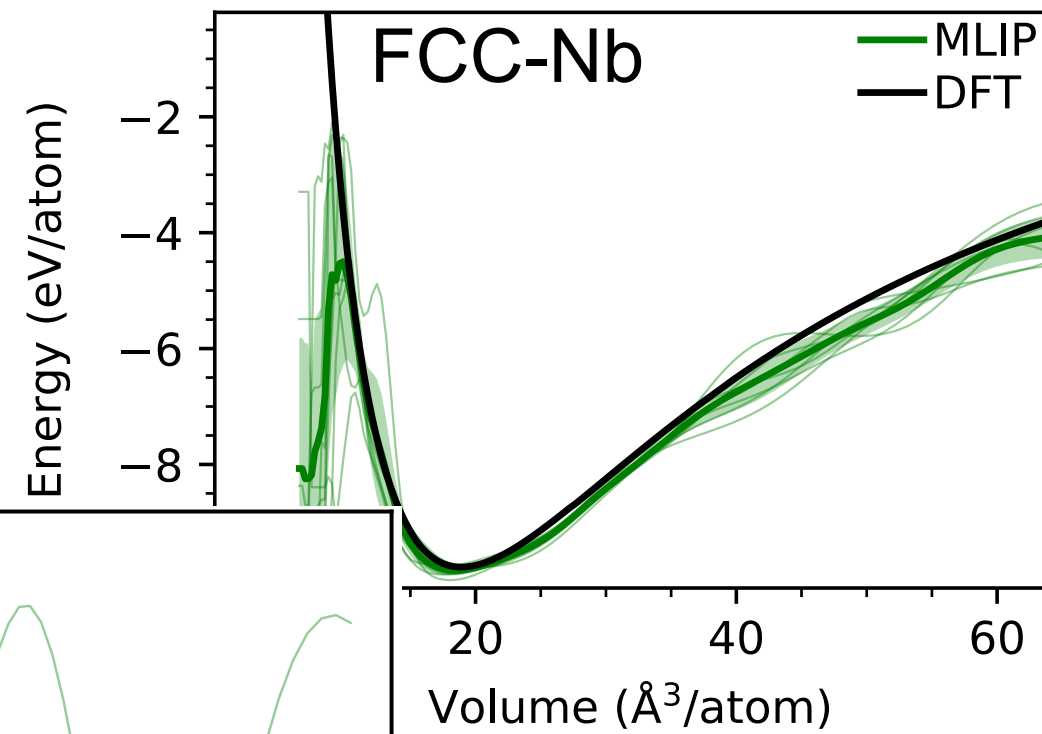
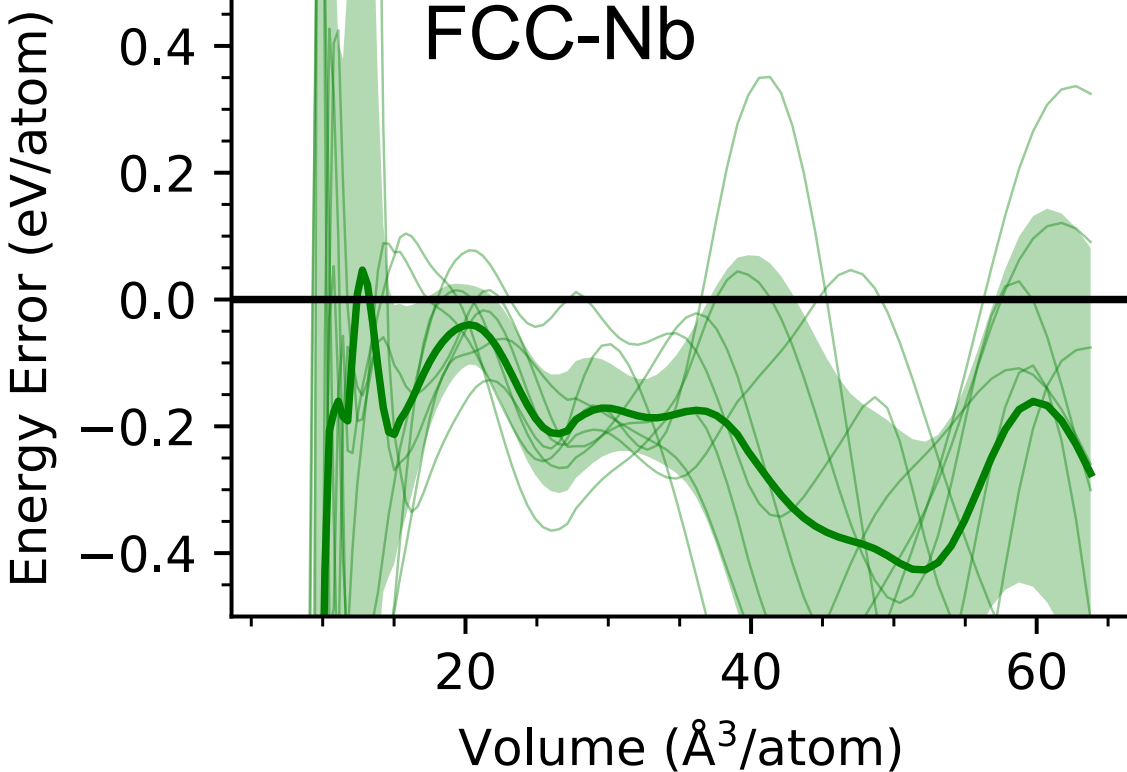
²van der Oord, C., Sachs, M., Kovács, D.P. et al.. npj Comput Mater 9, 168 (2023). <https://doi.org/10.1038/s41524-023-01104-6>

³Kulichenko, M., Barros, K., Lubbers, N. et al.. Nat Comput Sci 3, 230–239 (2023). <https://doi.org/10.1038/s43588-023-00406-5>

⁴Yoo, D., Jung, J., Jeong, W. et al. npj Comput Mater 7, 131 (2021). <https://doi.org/10.1038/s41524-021-00595-5>

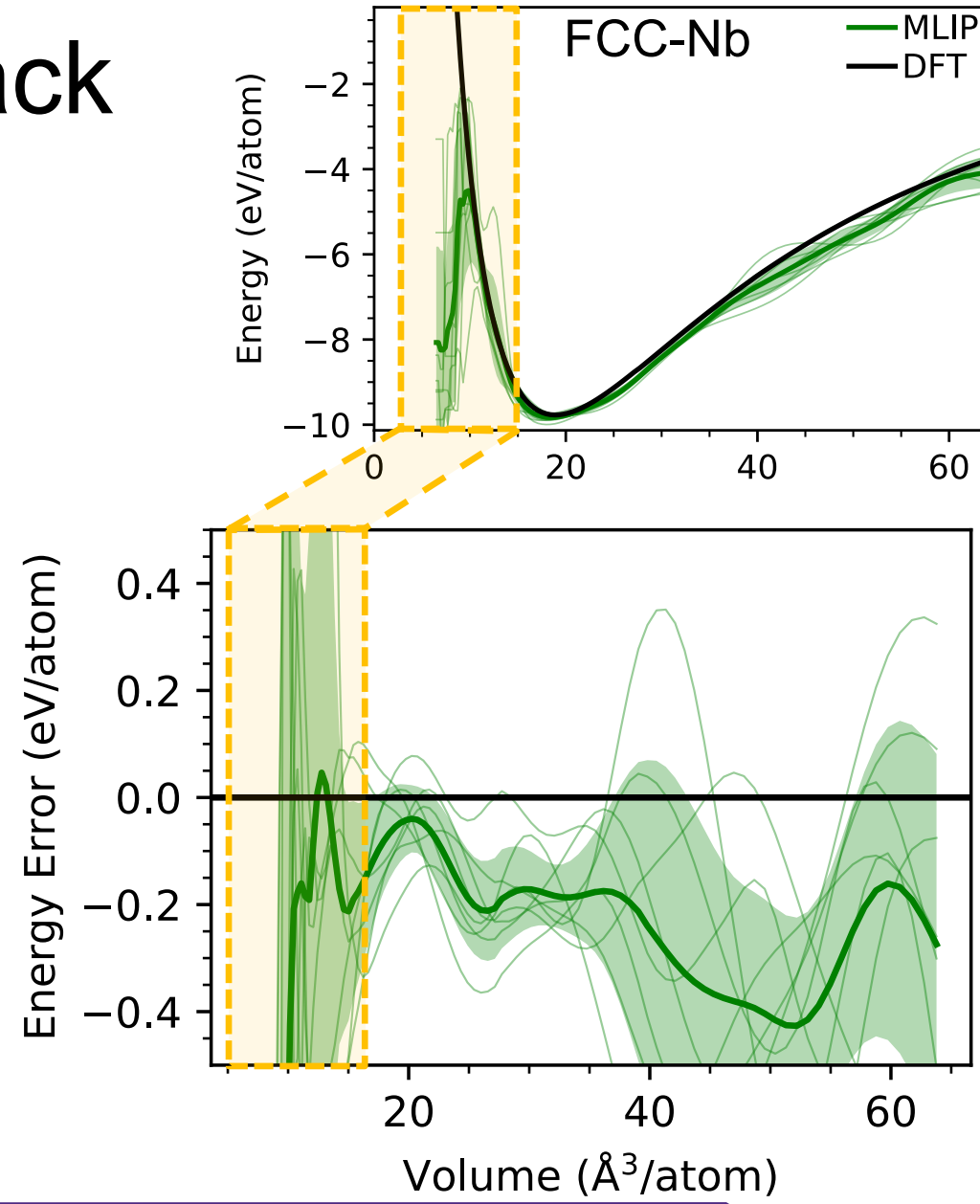
Committee MLIP Example

- **BCC-Nb** in training set
- **FCC-Nb** wasn't in the training set



Adversarial Attack

- Maximize uncertainty $\sigma_U(\mathbf{r})$ with respect to atom positions
 - Follow uncertainty gradient $\nabla\sigma_U(\mathbf{r})$
- **Will create many worthless structures**
 - The local maxima $\sigma_U(\mathbf{r})$ tend to have unphysical atom overlap and extreme energies



Adversarial Bias Schemes

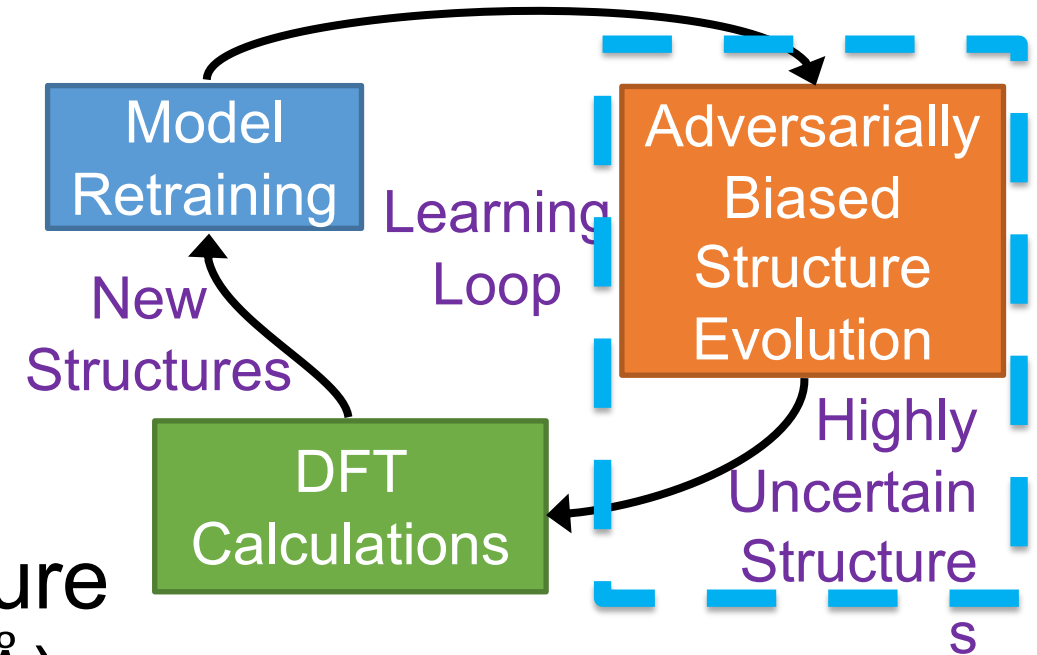
- **Schemes 1+2.** Add uncertainty potential wells
 - **Structure relaxation**
 - **Molecular dynamics**
- **Schemes 3.** Steer contour tangent, \hat{T} , with uncertainty gradient: $\hat{\nabla}\sigma_U$
 - **Contour exploration**
- α, γ unitless mixing parameters
 - If $\alpha, \gamma = 0$, \rightarrow active learning

$$U_{\text{total}} = \bar{U} - \alpha\sigma_U$$
$$F_{\text{total}} = \bar{F} + \alpha\nabla\sigma_U$$

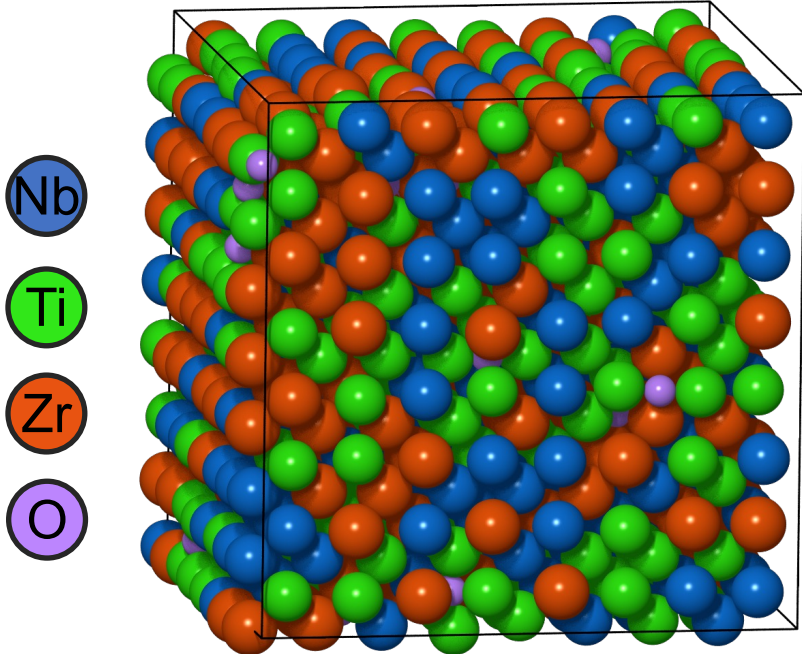
$$\hat{T}_{bias} = \gamma\hat{\nabla}\sigma_U + (1 - \gamma)\hat{T}$$

Testing Schemes

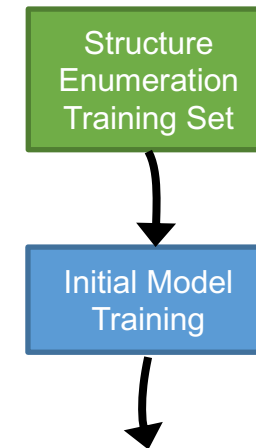
- *With and Without AdvB :*
 - Contour exploration (**CE**)
 - Molecular dynamics (**MD**)
 - Relaxation (**Relax**)
- Run structure evolution, pick structure with largest σ_U and $F < F_{\max}$ (25 eV/Å)
 - More unphysical atom overlap prevention



Target Application and Initial Data/Model

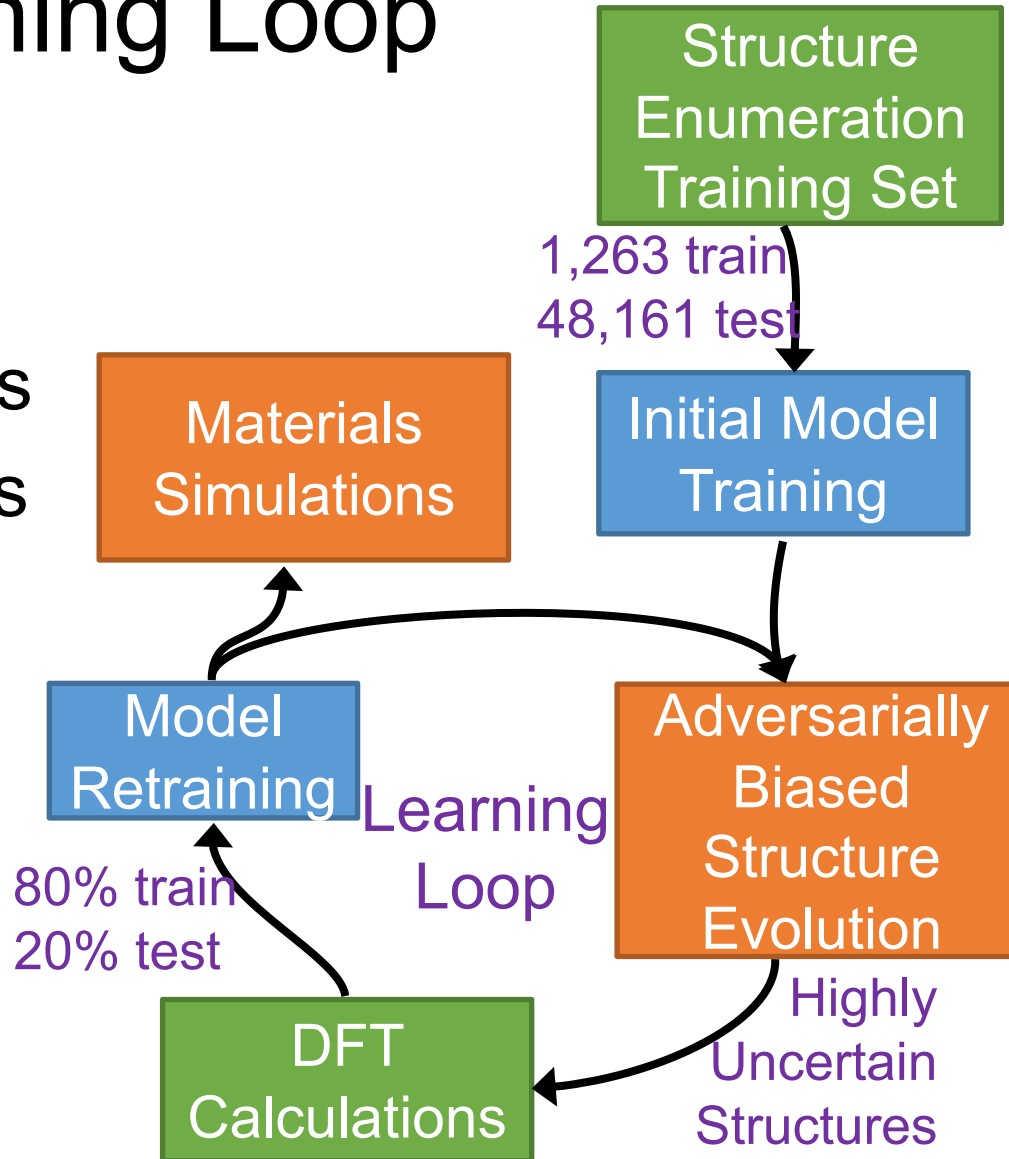


- BCC $\text{NbTiZr}+\text{O}_i$ model system for oxidation of Multi-principal element alloy (MPEAs)
- Many phases/polymorphs → challenging
- Key transport mechanisms
 - Oxygen interstitial (O_i) diffusion
 - Metal vacancy diffusion
- Initial Data: BCC $\text{NbTiZr}+\text{O}_i$ structure enumeration
 - 1,205 relaxation trajectories of unique permutations
 - Not robust training data
- *Which schemes most quickly generalize this MLIP?*



New Structures and Learning Loop

- New structures per loop:
 - 50 Derived structures from metal phases
 - 50 Derived structures from oxide phases
 - 100 Random structures
 - 20% reserved for **difficult** test set
- Remaining relaxation trajectory data → **gentle** test set

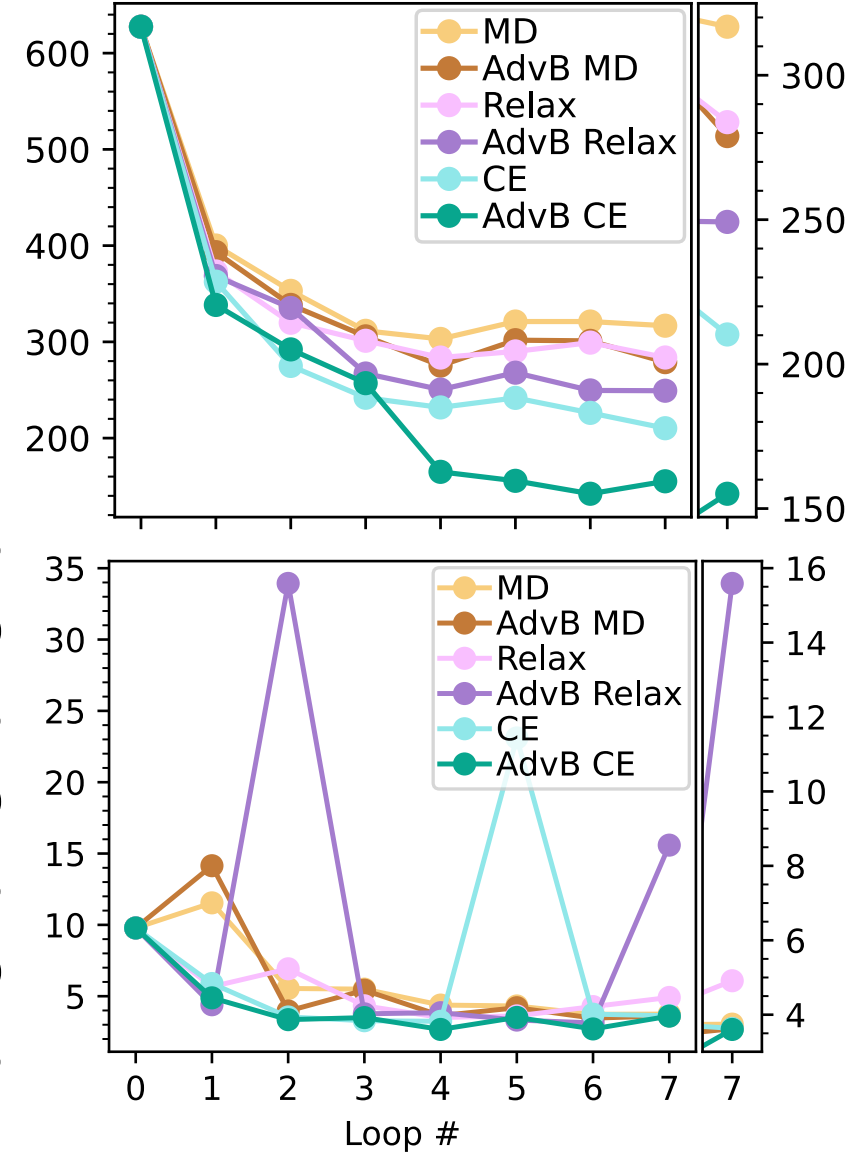
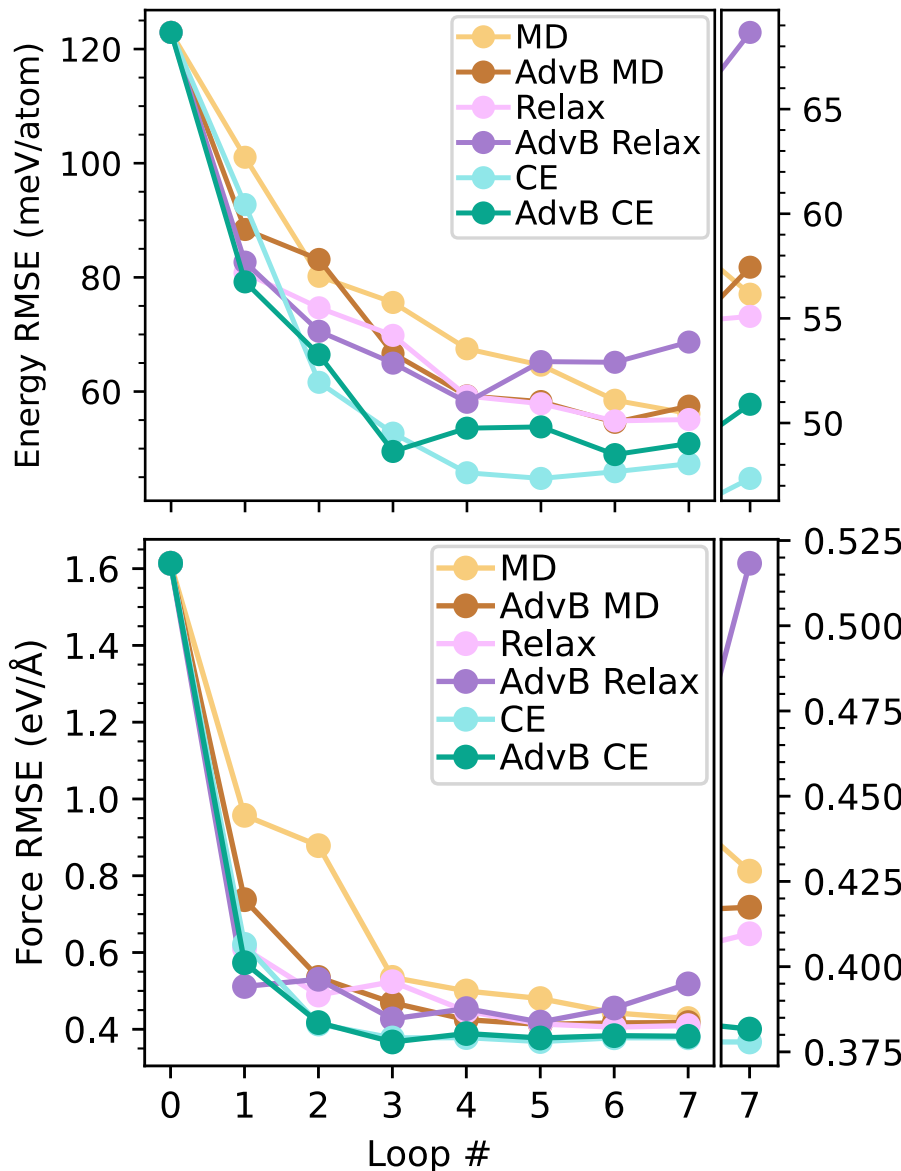


Statistical Performance

Gentle

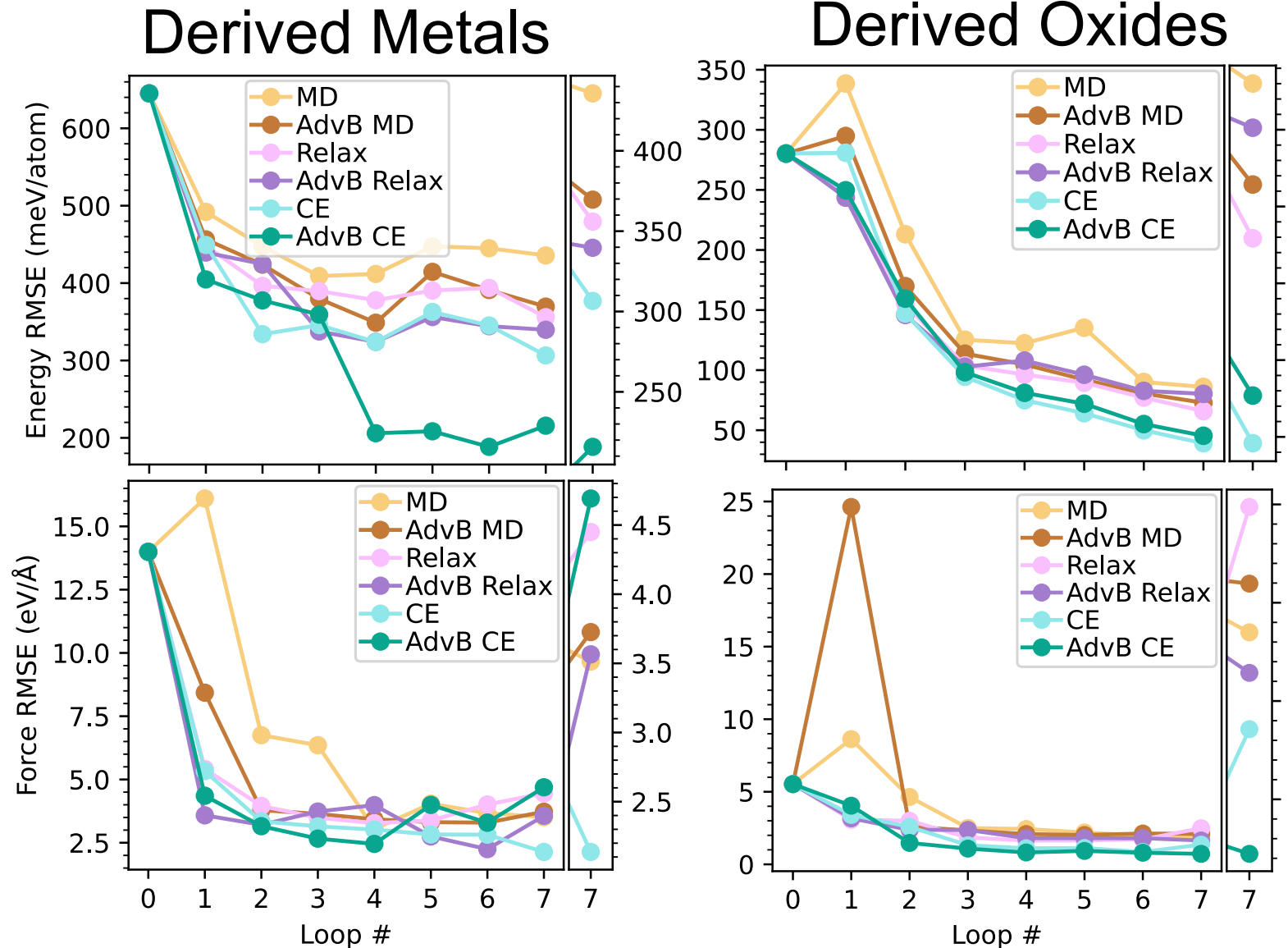
Difficult

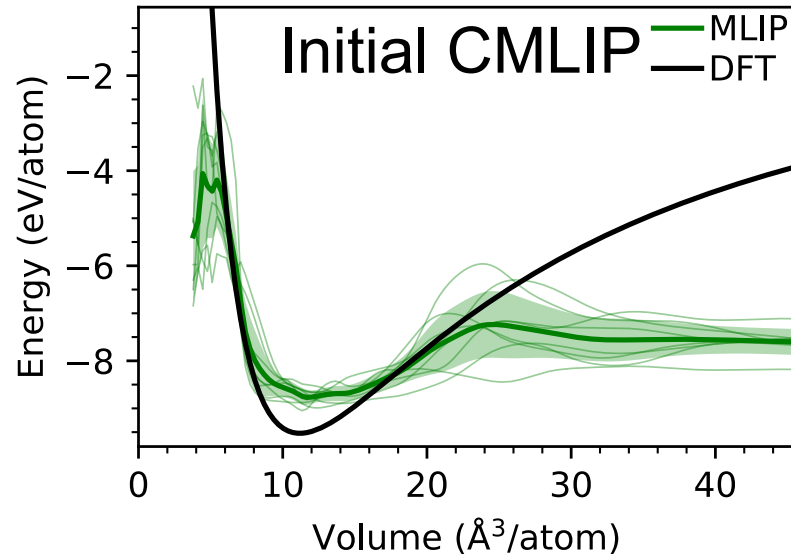
- All methods show improvement
- CE/AdvB CE generally have best improvements
- AdvB relaxation works well early on
 - α too small afterwards?



Difficult Set: Performance by Structure Type

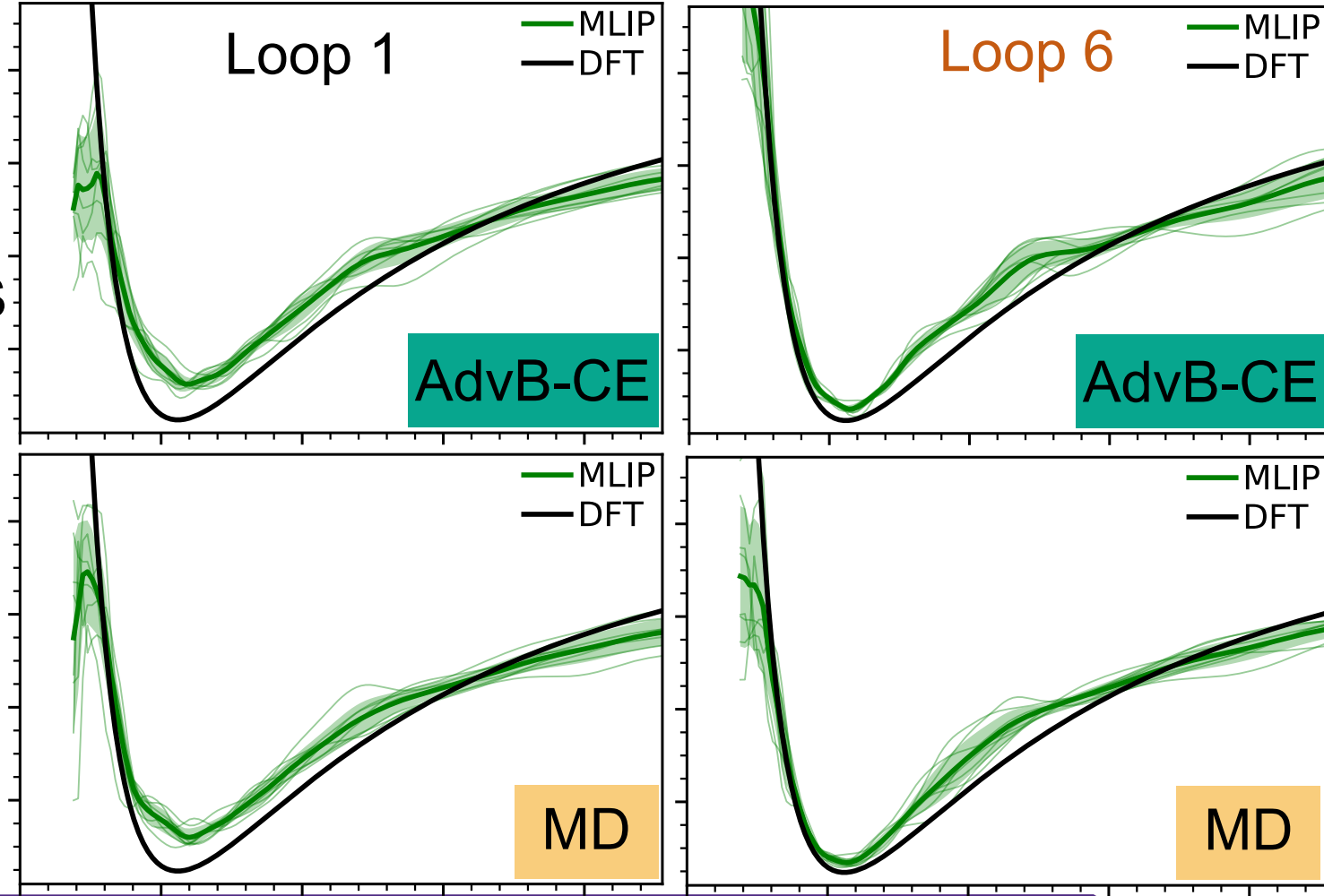
- Surprisingly high error on metals
- Surprisingly low error on oxides
 - Only ≈ 32 new derived oxide structures per loop





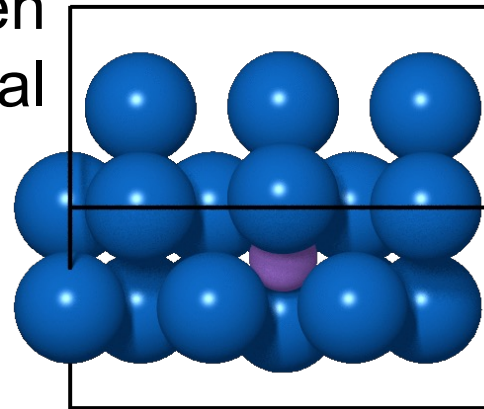
c-ZrO₂

- Best and worst for oxides
- 1 Loop to qualitatively correct!
- Minima seems to be challenging
 - Tried lower $F_{\max} = 2 \text{ eV}/\text{\AA}$ in loop 6, 7

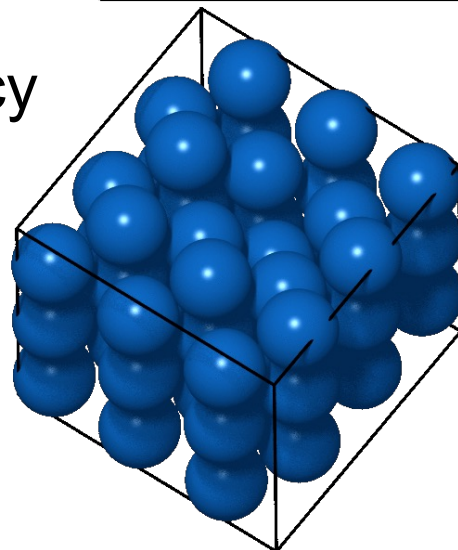


Diffusion Barriers

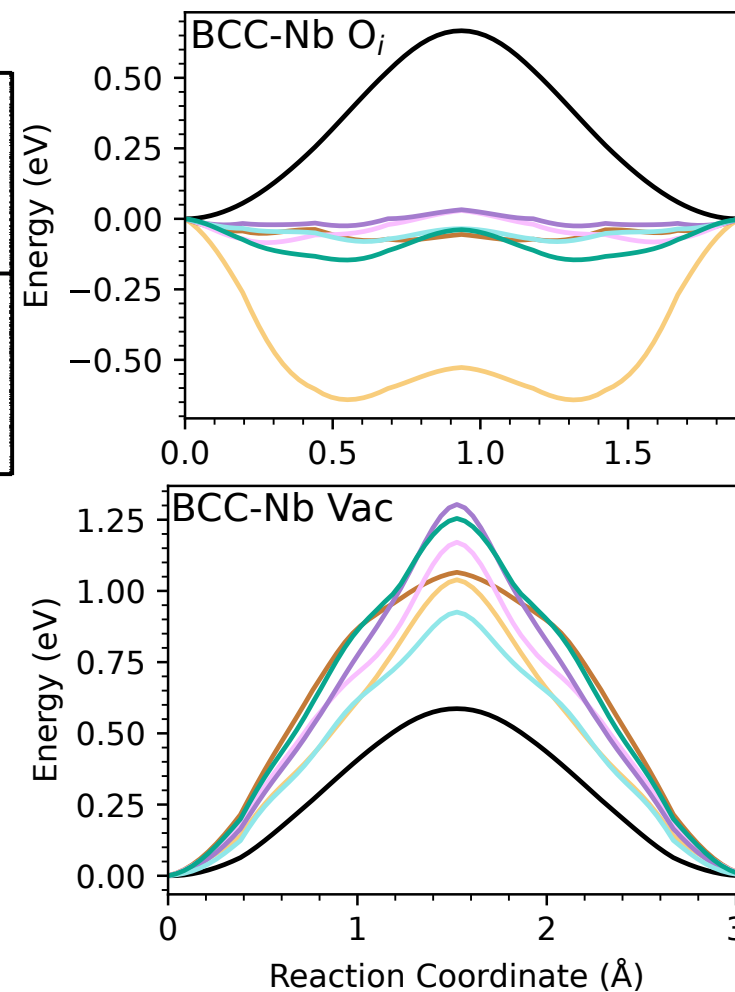
Oxygen
Interstitial



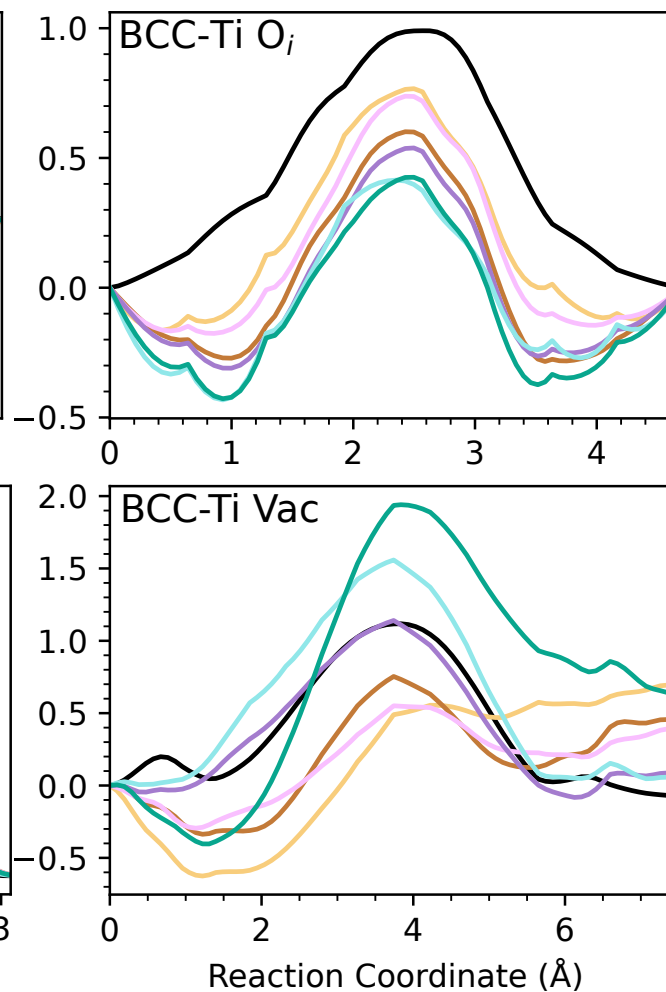
Vacancy



Nb



Ti

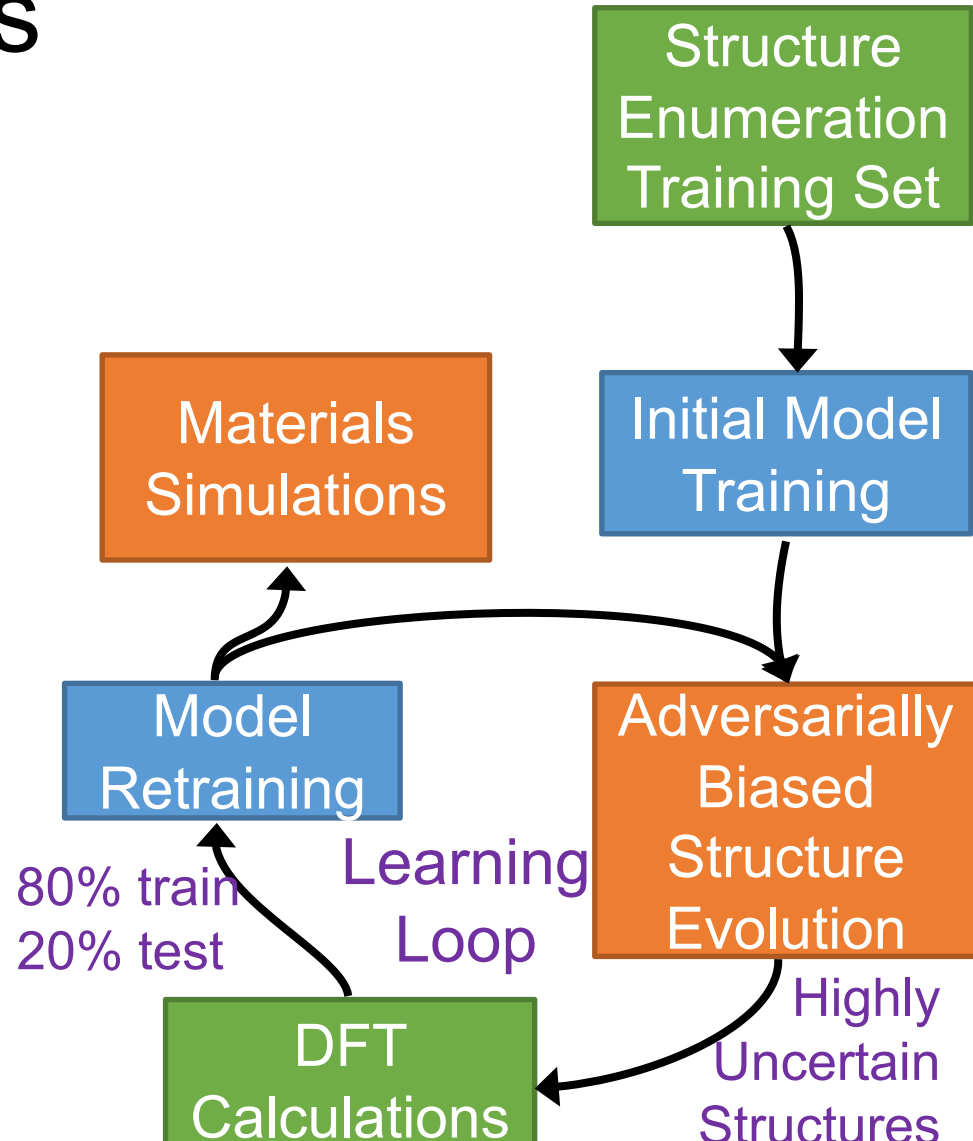


- DFT
- MD
- AdvB MD
- Relax
- AdvB Relax
- CE
- AdvB CE

- No outstanding performances

Conclusions

- Demonstrated new adversarially biased structure evolution scheme(s)
 - Adversarial bias schemes typically better than active learning equivalents
 - Contour exploration with and without adversarial bias gave best learning improvements
 - Diffusion barriers were difficult

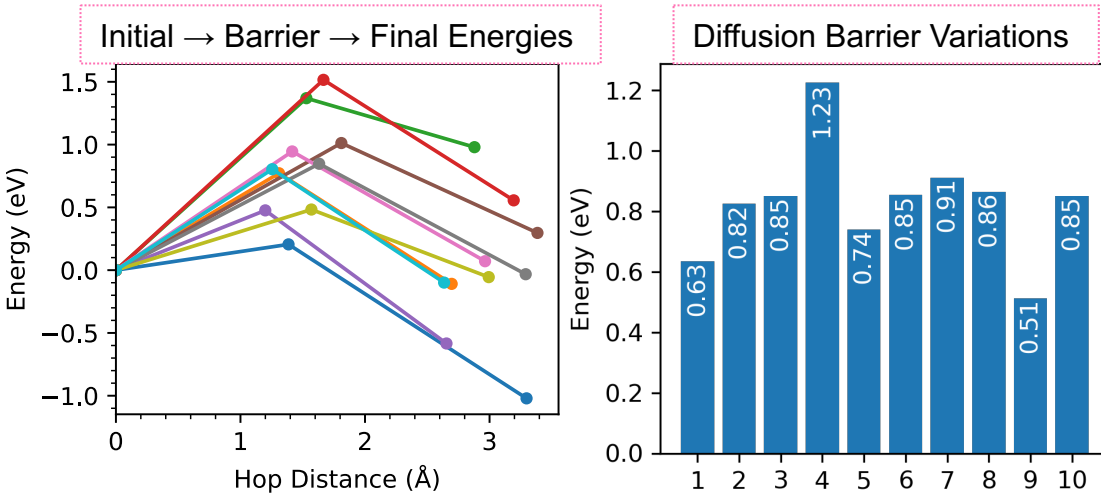


Active barrier learning

What does diffusion look like in an MPEA?

Sampling Diffusion Pathways in Random NbTiZr at the DFT Level

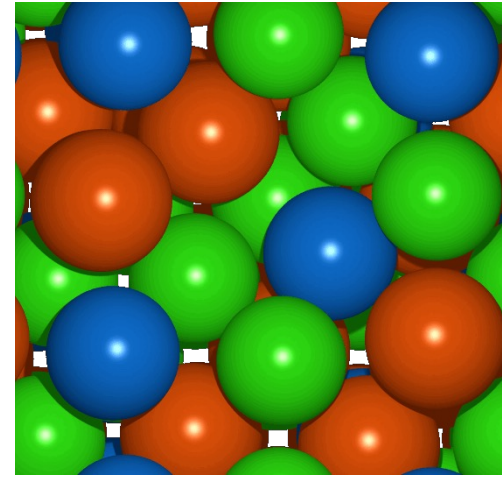
Oxygen Interstitial Diffusion in NbZrTi



For oxygen interstitials:

- Site energy variations
- Non-uniform barriers even when subtracting the site energy changes

Coupled vacancy hopping in NbTiZr

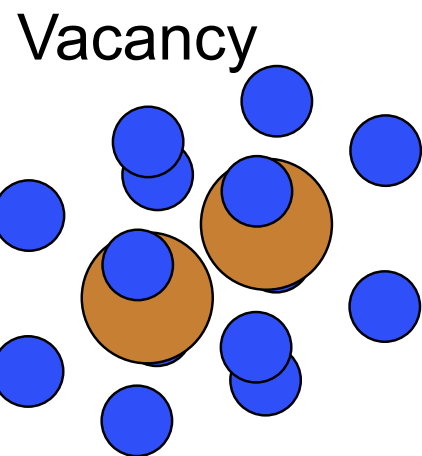
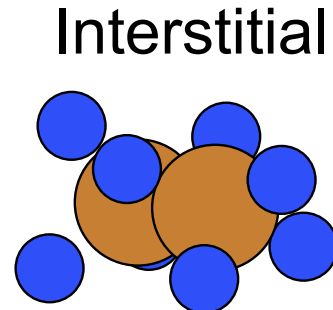


Metal vacancy diffusion more complex:

- Some atoms coupled vacancy hopping
- Some atoms prefer to sit between sites

Diffusivity in MPEAs is an aggregate over many local chemical environments

Challenging Permutations

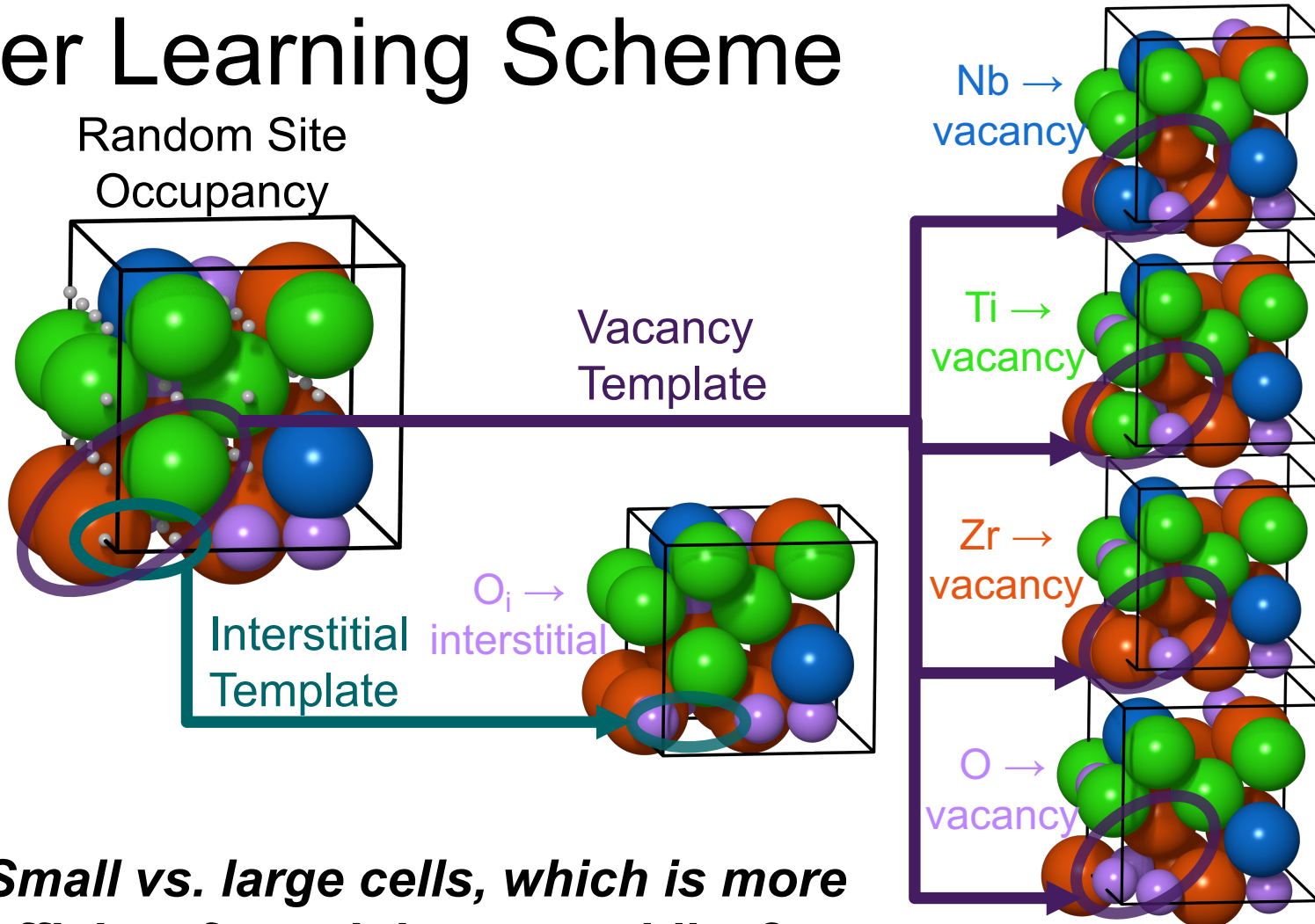
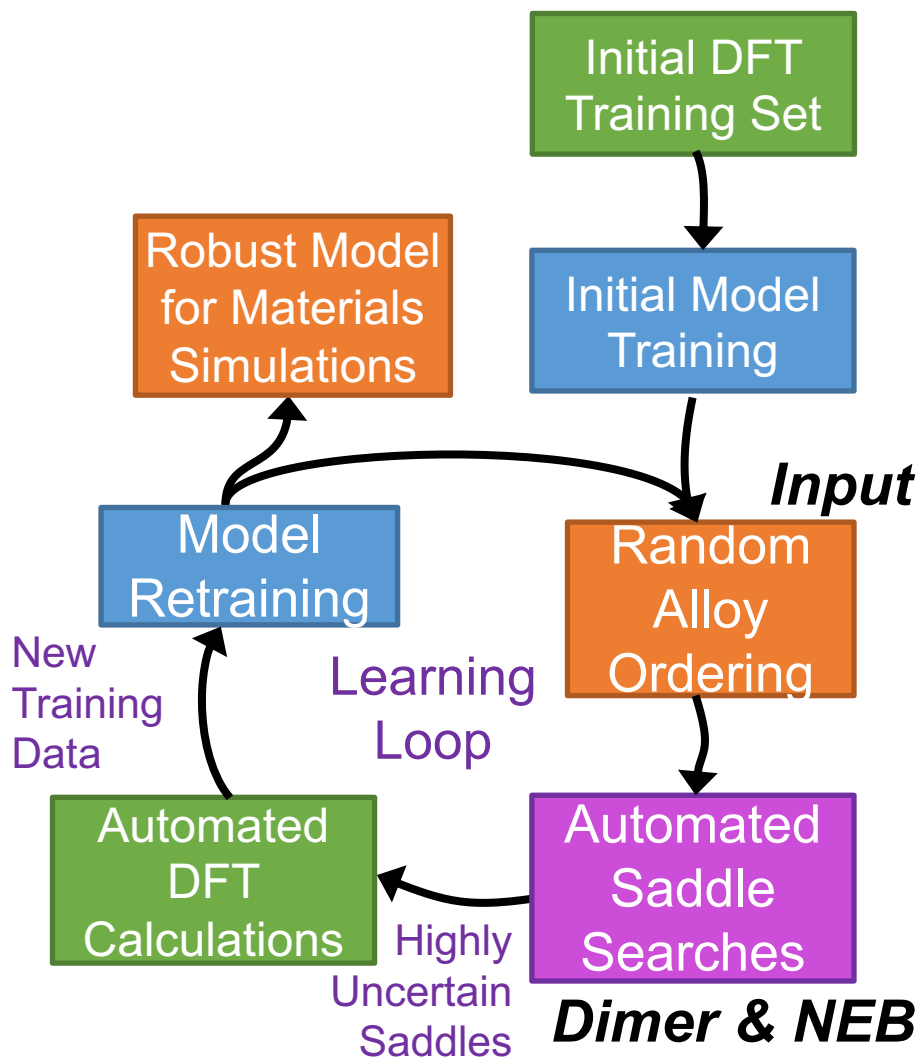


3-Component BCC Diffusion Pathways

	# Path NN	# Unique Neighbor Permutations
Interstitial	8	1035
Vacancy	14	826,929 ($\times 3$ metals) = 2,480,787

- Active barrier learning → a practical means of studying the kinetics of MPEAs?

Active Barrier Learning Scheme

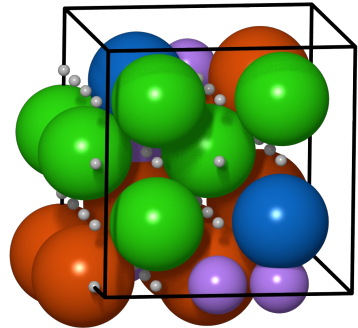


Small vs. large cells, which is more efficient for training on saddles?

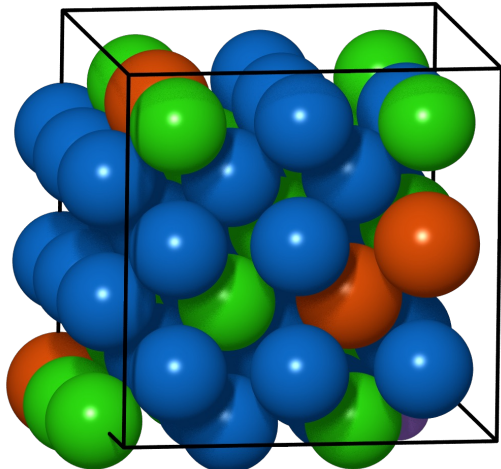
- More saddle point atoms involved per small cell
- Less bulk-like behavior
- Cell sizes are a hyperparameter

Cell Morphology as a Hyperparameter

2x2x2

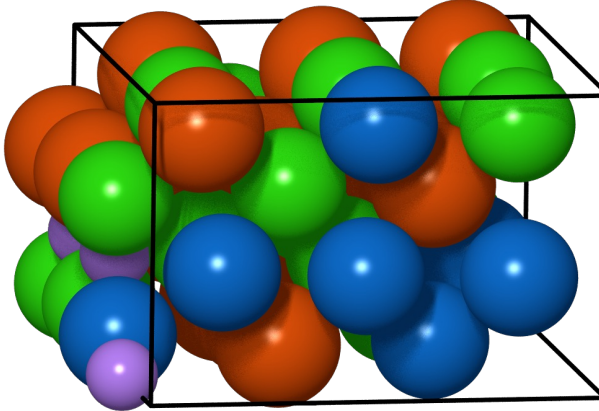


3x3x3



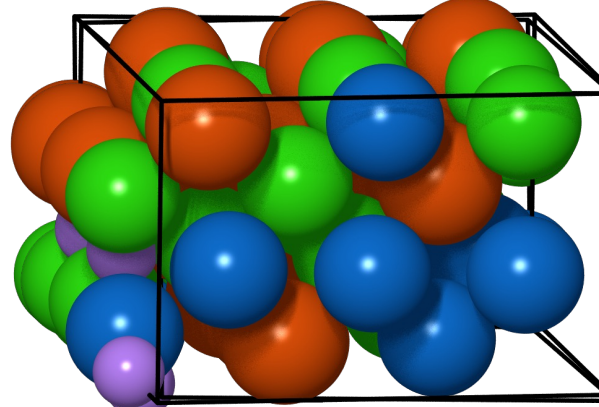
Mix of 2-3x

- Random in each direction:
- $N_1 \times N_2 \times N_3$ ($N_i = 2$ or 3)
- Ex.: $3 \times 2 \times 3$



Mix of 2-3x + random strain

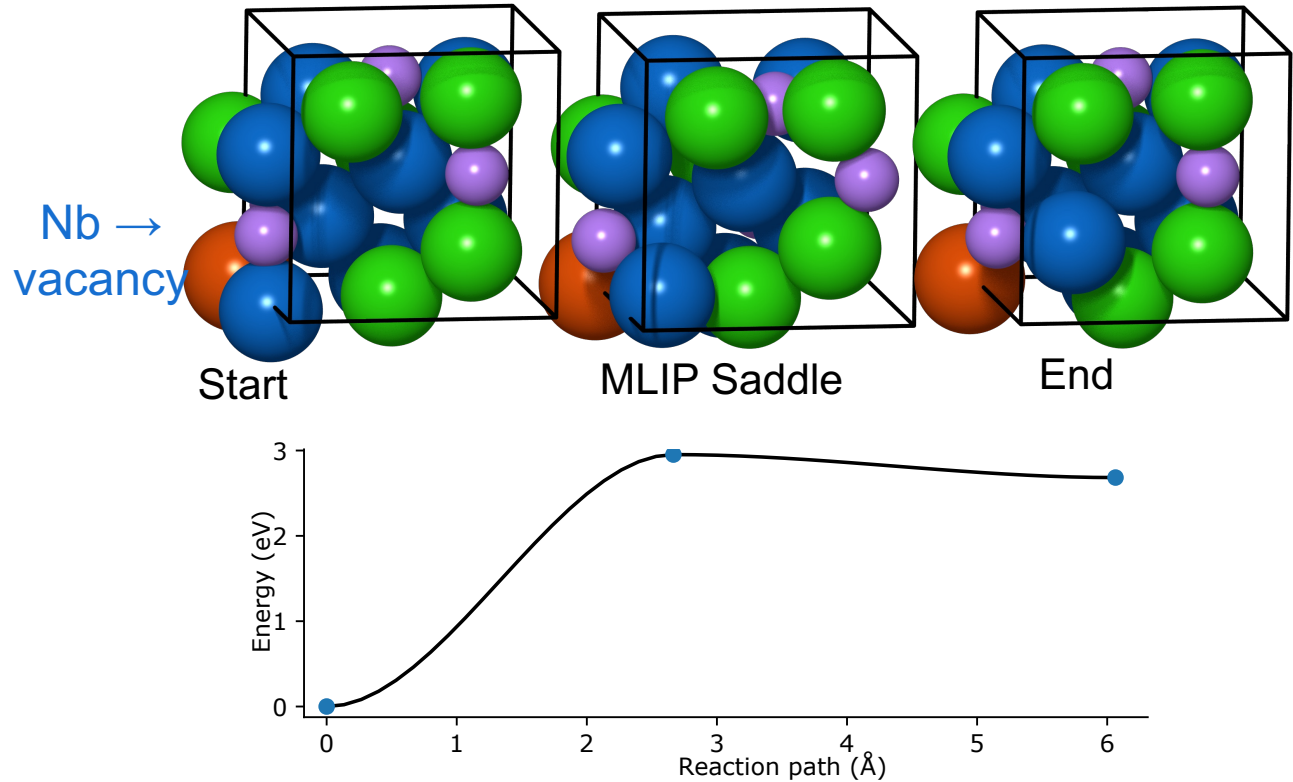
- Emulating lattice strain in complex alloys
- Uniform linear strain (-5% to +10%)
- Von Mises strain (0 to 5%)



Automating Saddle Searches

Saddle search steps:

1. Relax start and end
2. Interpolate and perform dimer search for saddle
3. NEB±CI if dimer fails

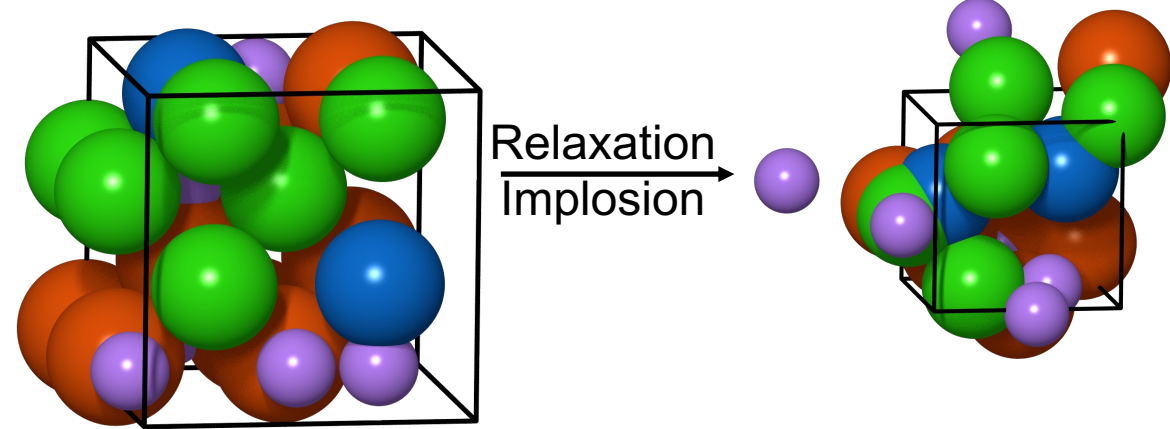
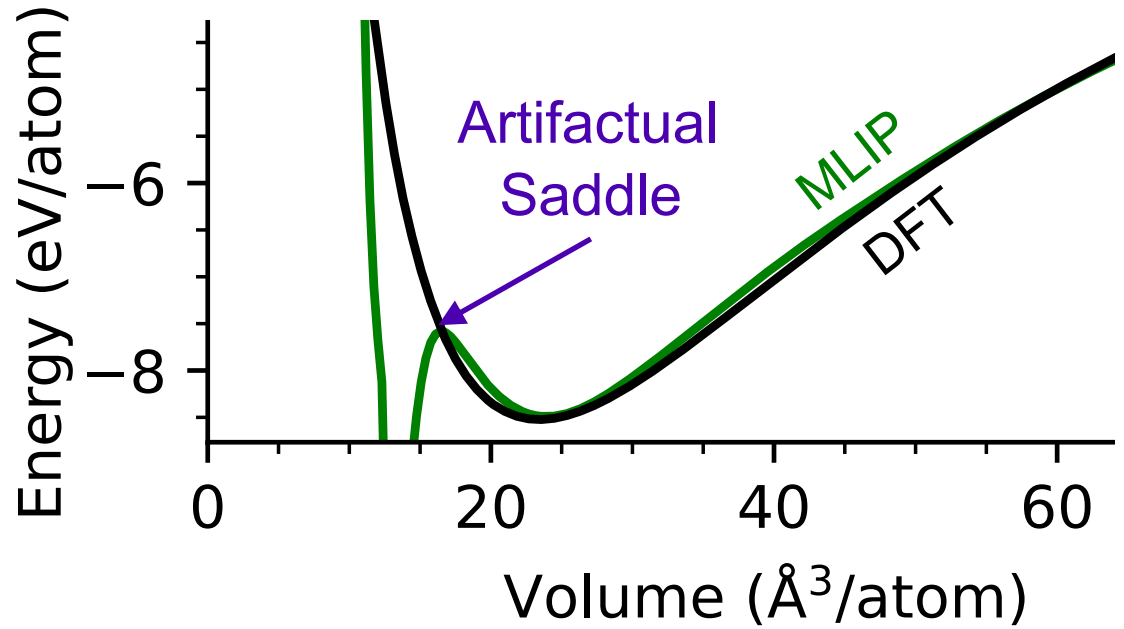


MLIP saddles are not true saddles due to error

- MLIP saddle is near a true saddle (**proximal saddles**)
- MLIP saddle is unphysical (**artifactual saddles**)

Automating Saddle Searches

A great way to find instabilities



Artifactual Saddles

- DFT reveals high forces \rightarrow artifactual saddle
 - Threshold: $F_{\max} > 2 \text{ eV}/\text{\AA}$
- Add to training set to correct PES

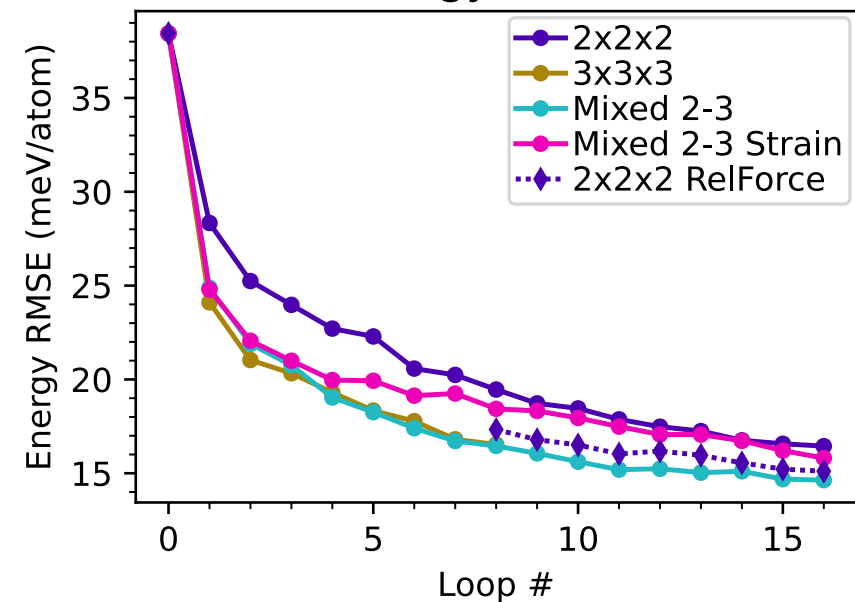
Instabilities During Relaxation

- Add initial structures that fail to relax to training set
 - Small number

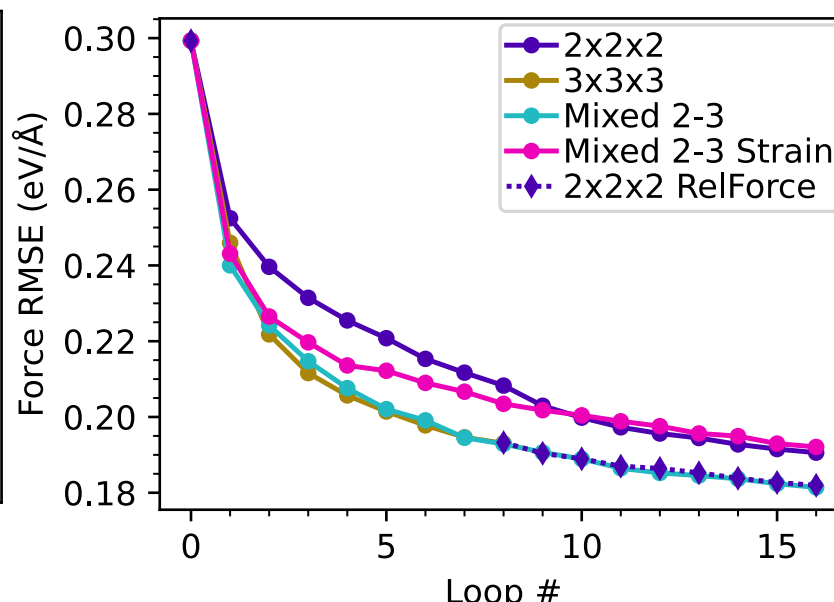
Learning Performance 1

MLIP Proximal Saddle Test Set

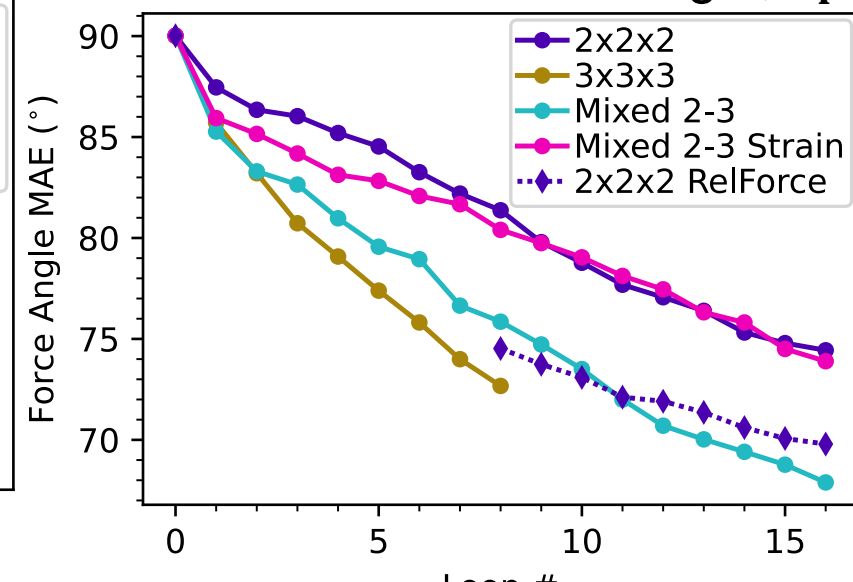
Energy Error



Force Error



Force Vector Error Angle, θ_F



- Force and energy errors are acceptable
- But, ($\mathbf{F} \rightarrow 0$) at saddle points
 - force direction error more diagnostic
- Force direction error \rightarrow slow systematic improvement
- Implemented relative force weighting at loop 9

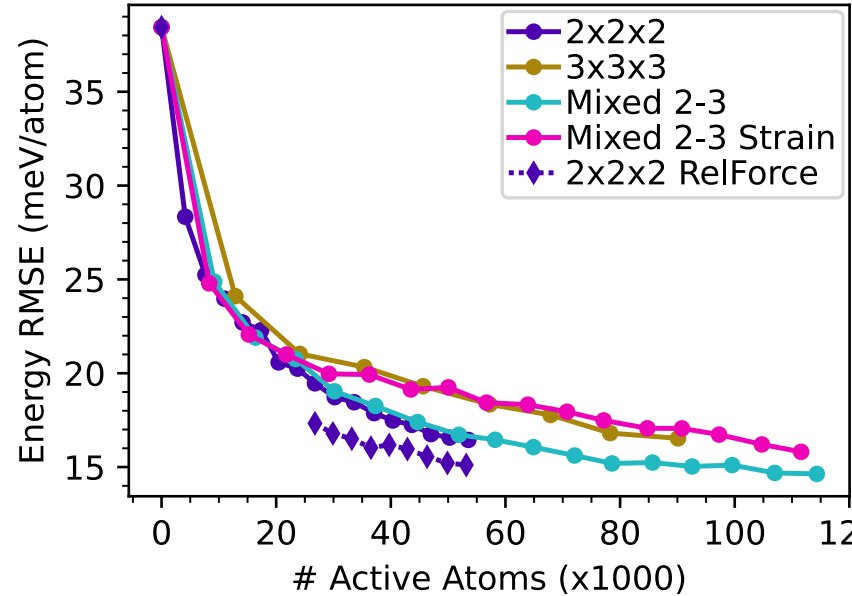
$$\theta_F = \cos^{-1} \left(\frac{\mathbf{F}_{MLIP} \cdot \mathbf{F}_{DFT}}{|\mathbf{F}_{MLIP}| |\mathbf{F}_{DFT}|} \right)$$

$$L_{\mathbf{F}} = \sum_i^{N_{atoms}} \left(\frac{1}{|\mathbf{F}_{DFT}|^2 + \varepsilon} \right) |\mathbf{F}_i - \mathbf{F}_{DFT}|^2$$

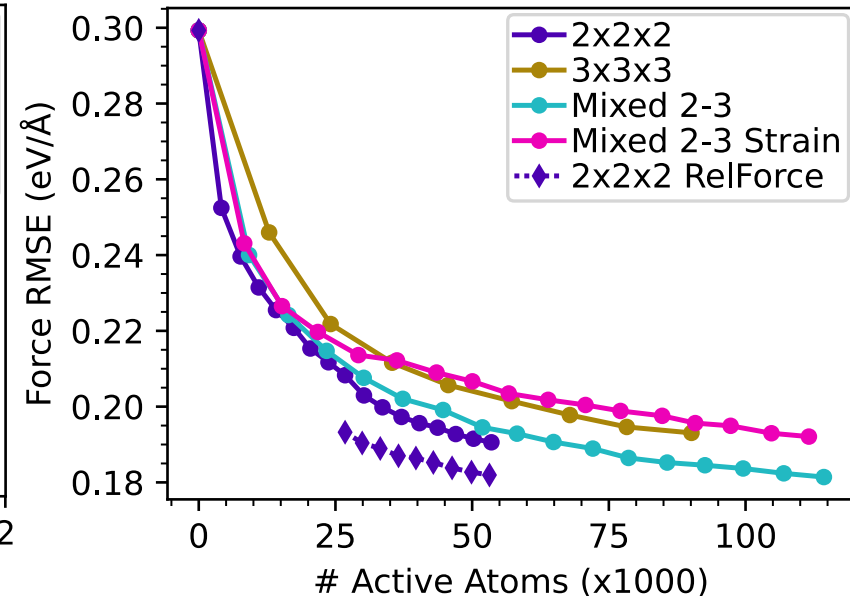
Learning Performance 2

MLIP Proximal Saddle Test Set

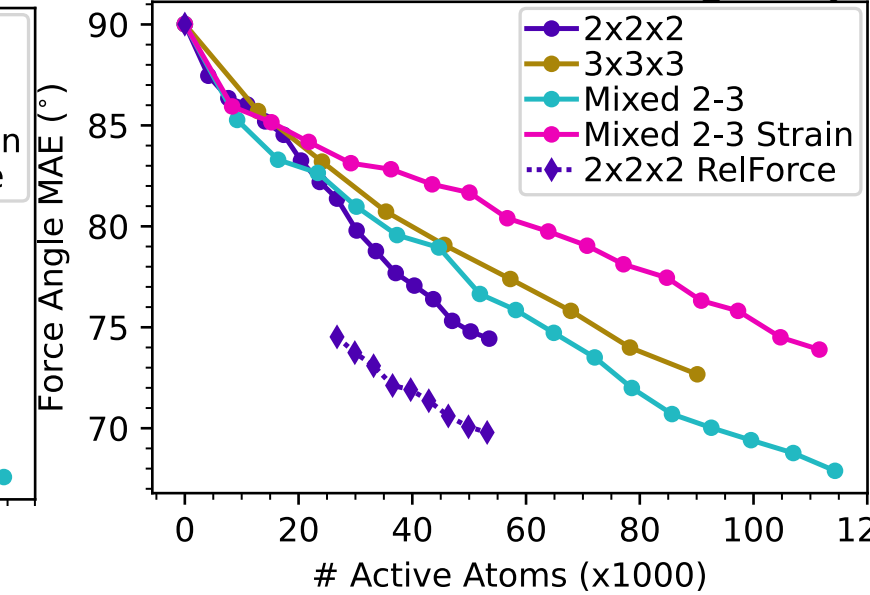
Energy Error



Force Error



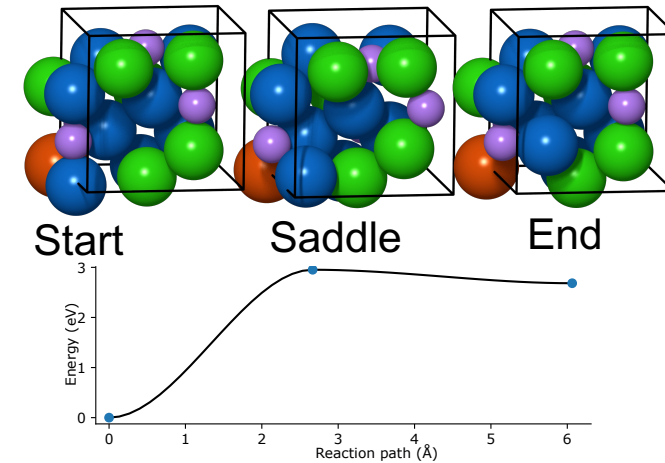
Force Vector Error Angle, θ_F



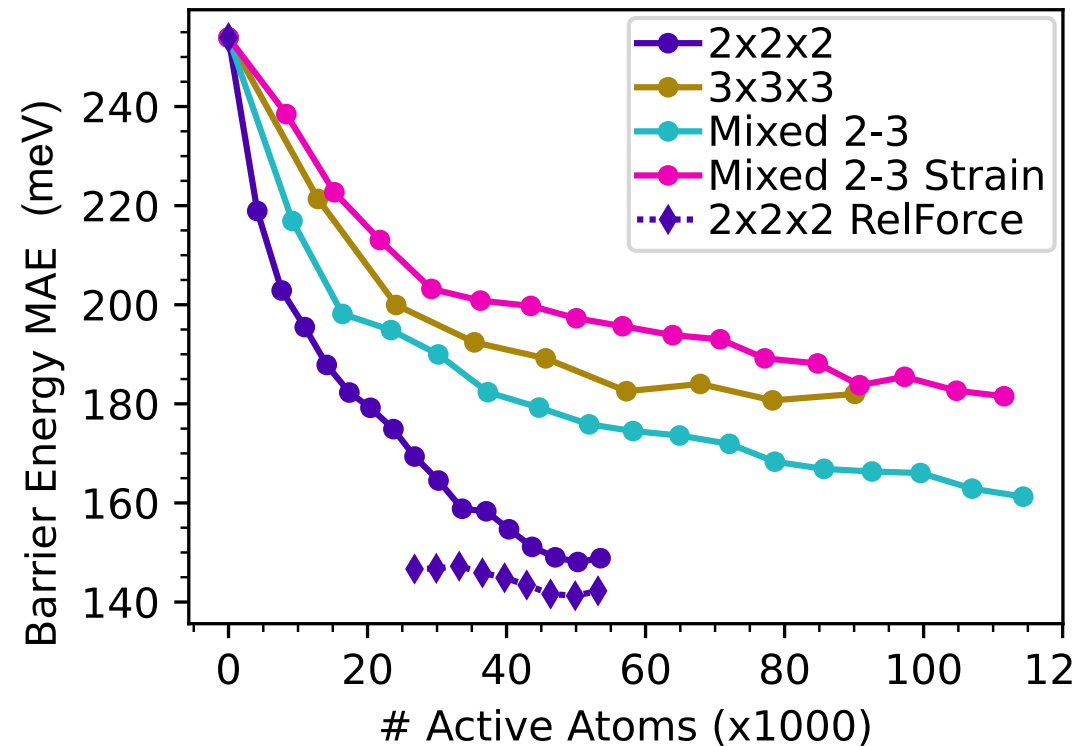
- Larger cells lag in learning improvement *per atom*
 - Significant considering $O(n^3)$ scaling of computational cost!

Learning Performance 3

- Actively selected structures are unrealistically challenging
- Random set of *start-saddle-end* DFT calculations created
 - 2x2x2
 - 3x3x3 → Still running

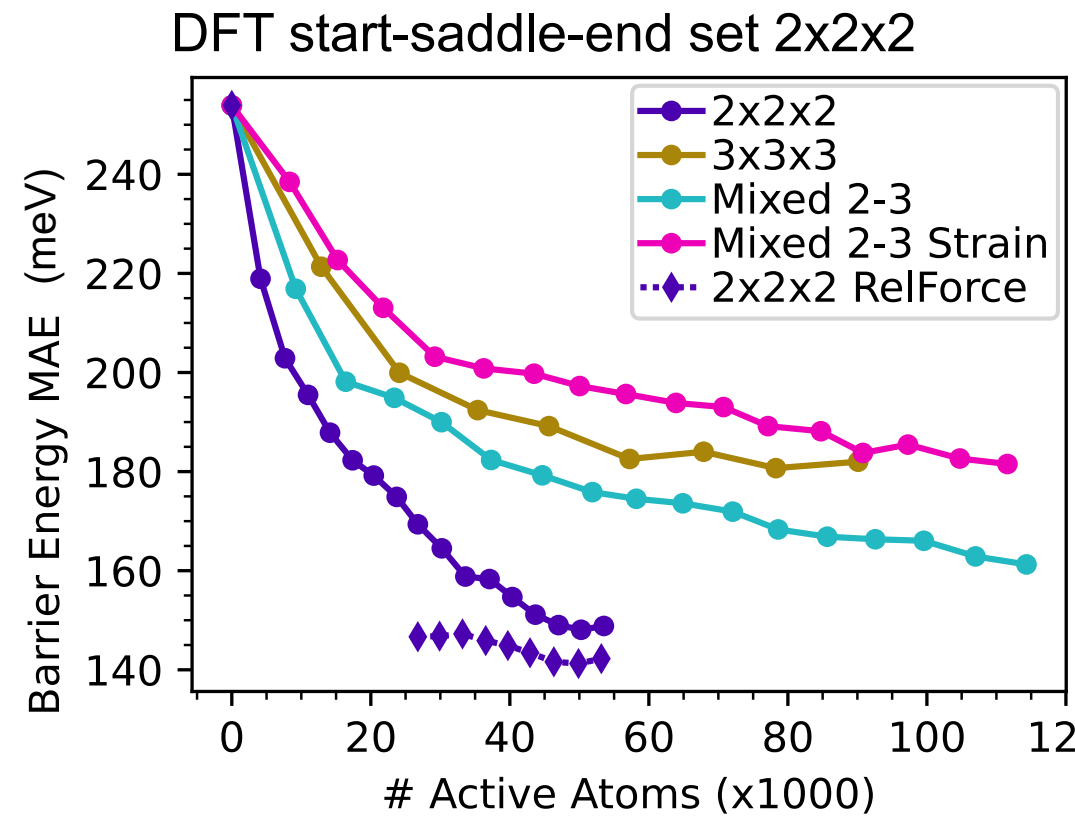


DFT start-saddle-end set 2x2x2



Conclusions

1. Active learning of diffusion barriers looks to be a practical means of treating MPEA kinetics
2. Small cells are more efficient
 - Huge when considering DFT costs!
3. Relative force weighting improves accuracy



Acknowledgements

The Rondinelli Group



Funding is provided by the Office of Naval Research award N00014-20-1-2368 and N00014-16-1-2280

Our research uses resources of the National Energy Research Scientific Computing Center (NERSC), a DOE Office of Science User Facility supported by the Office of Science of the U.S. Department of Energy under Contract No. DE-AC02 -05CH11231 using NERSC award BES-ERCAP0028012, ERCAP0020980, ERCAP0017517



National Energy Research
Scientific Computing Center

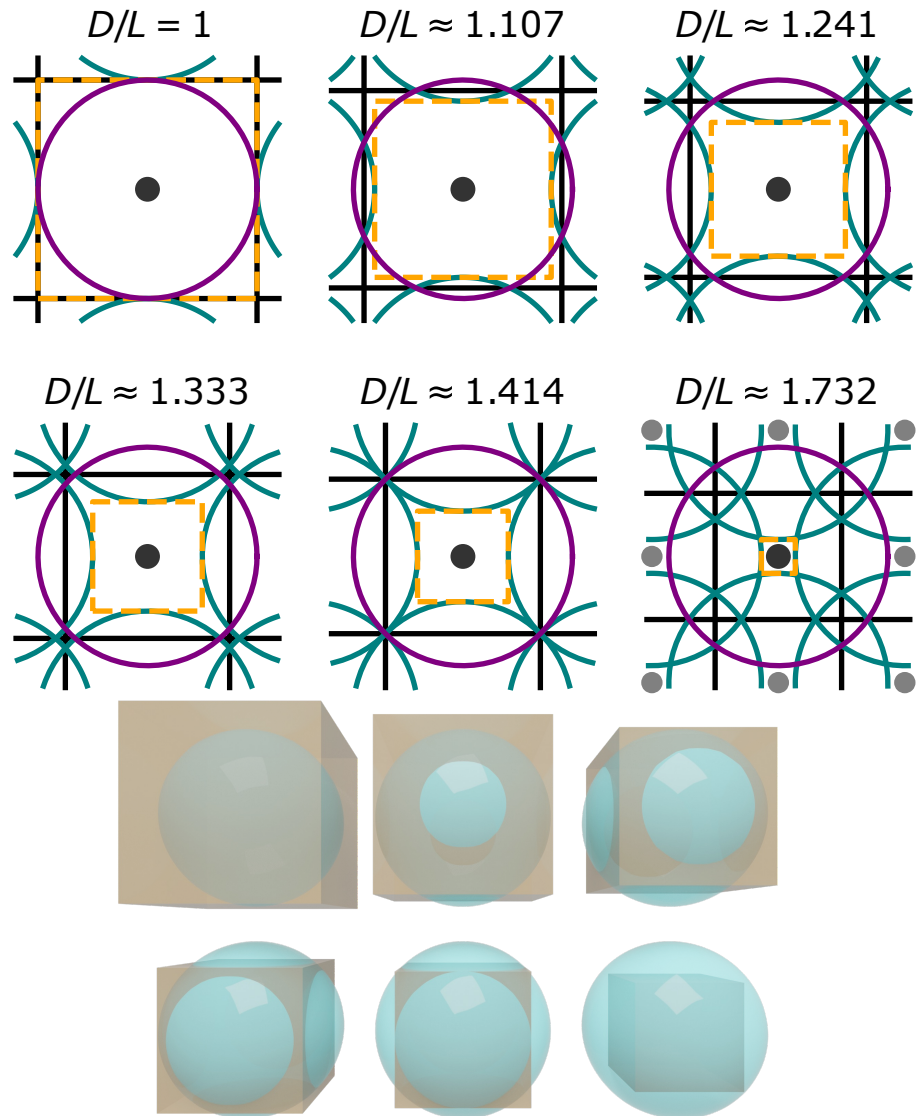
Extra Slides 1

Cell Sizes and Spheres of Influence

- What fraction of a sphere of influence is periodic images?

Table S1: Various metrics for the uniqueness and cost of random structures taken from geometric considerations. The simulation cell sizes are given by edge length, L , the diameter of the sphere of influence (SOI) is D , and the SOI is the interaction volume defined by the interaction cutoff radius, r_{cut} such that $D = 2r_{cut}$. An inscribed sphere has $D = L$.

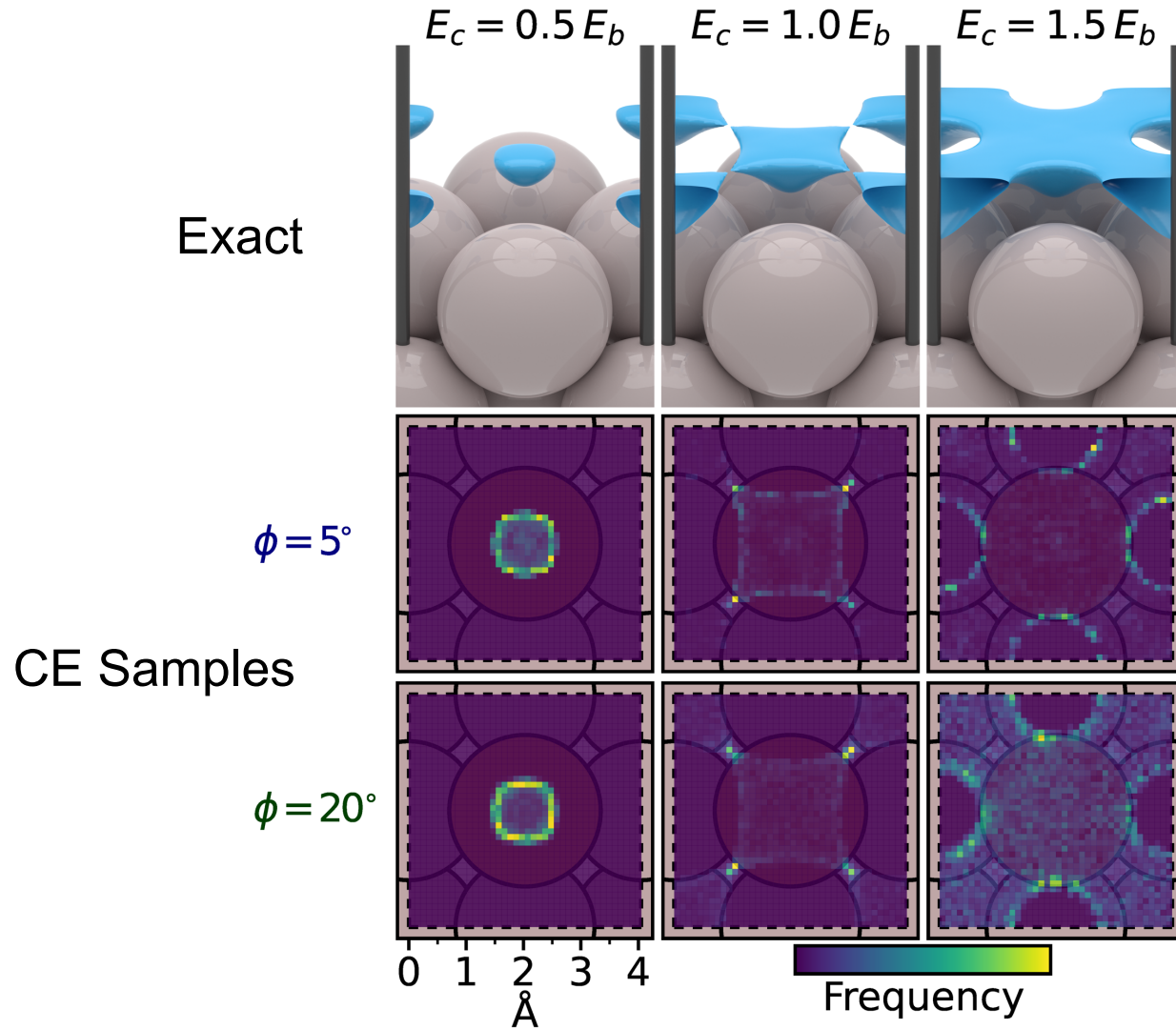
Geometric Description	Diameter Length	Metrics (Descriptor Ratios)			
		(a) SOI Volume / Cell Volume	(b) Unique Radius / Cutoff Radius	(c) Unique Volume / SOI Volume	(d) Relative Cell Volume
Inscribed Sphere	1	$\pi/6 \approx 0.524$	1	$6/\pi \approx 1.910$	1
Unique volume = SOI volume	$\frac{2}{(\frac{\pi}{6})^{\frac{1}{3}} + 1} \approx 1.107$	$288\pi / (\pi^{\frac{1}{3}} 6^{\frac{2}{3}} + 6)^3 \frac{6^{\frac{2}{3}} \pi^{\frac{1}{3}}}{6}$		1	$(\pi^{\frac{1}{3}} 6^{\frac{2}{3}} + 6)^3 / 1728$
Cell volume = SOI volume	$(\frac{6}{\pi})^{\frac{1}{3}} \approx 1.2407$	1	$\frac{6^{\frac{2}{3}} \pi^{\frac{1}{3}}}{3} - 1$	$\frac{(2\pi^{\frac{1}{3}} - 6^{\frac{1}{3}})^3}{\pi}$	$\pi/6$
Inner half of r_{cut} is unique	$4/3 \approx 1.333$	$(\frac{4}{3})^3 \frac{\pi}{6}$	1/2	$\frac{3}{4\pi}$	$(\frac{3}{4})^3$
SOI touches cell edges	$\sqrt{2} = 1.414$	$\frac{\pi\sqrt{2}}{3}$	$\sqrt{2} - 1$	$\frac{30\sqrt{2} - 42}{\pi}$	$\frac{1}{(\sqrt{2})^3}$
SOI circumscribes cell	$\sqrt{3} = 1.732$	$\frac{\pi\sqrt{3}}{2}$	$\frac{2}{\sqrt{3}} - 1$	$\frac{52/\sqrt{3} - 30}{\pi}$	$\frac{1}{(\sqrt{3})^3}$



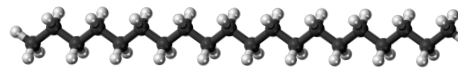
Extra Slides 2

Contour Exploration on a Surface

- Frozen Al surface
- EMT potential



MD, Metadynamics, and CE



- Benchmarking with *n*-Icosane
- CE → wider angle sampling, more general
- MTD → Better exploration of collective variables

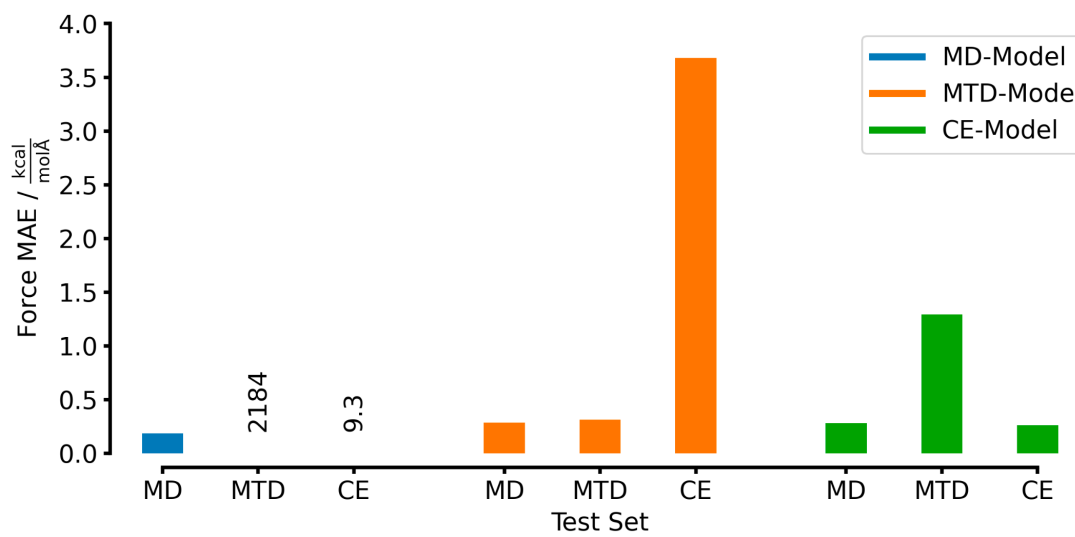


Figure 3.6: MAEs of the force prediction for models trained on the MD, MTD and CE trajectories of *n*-Icosane.

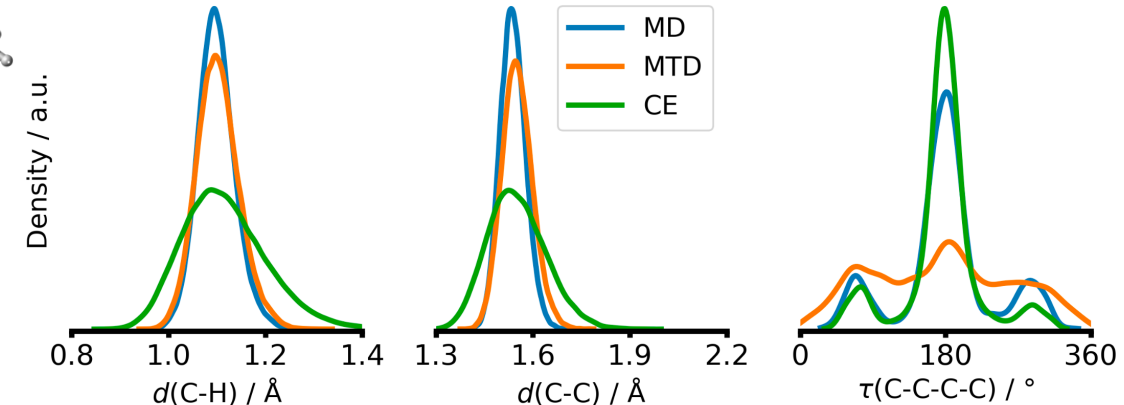


Figure 3.4: Distribution of C-H and C-C bond lengths as well as C-C-C-C torsion angles in the MD, MTD and CE trajectories of *n*-Icosane.

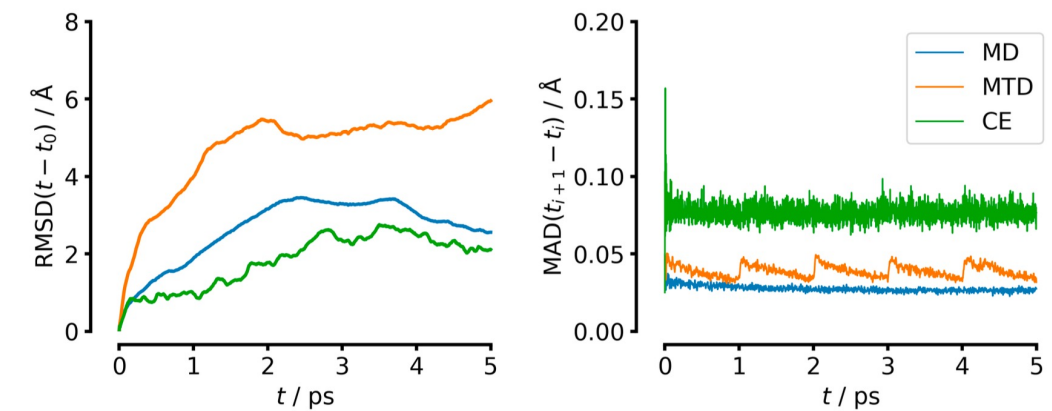


Figure 3.5: RMSD and magnitude of position updates for the MD, MTD and CE trajectories of *n*-Icosane.

Total Update Vector + Optional Drift

- We can add momentum drift to increase the space explored
 - Must be perpendicular to force and our tangent direction

$$\mathbf{N} \cdot \Delta\mathbf{r}_{drift} = 0 \quad \mathbf{T} \cdot \Delta\mathbf{r}_{drift} = 0$$

- The total update vector:

Potentiostat term,
Corrects contour
energy error

Contour following term

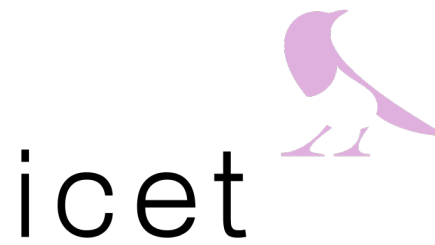
Drift term, fraction of
contour following step

$$\Delta\mathbf{r} = \boxed{\Delta\mathbf{r}_\perp} + \boxed{\Delta\mathbf{r}_\parallel(s)} + \boxed{\Delta\mathbf{r}_{drift}}$$

Extra Slides 3

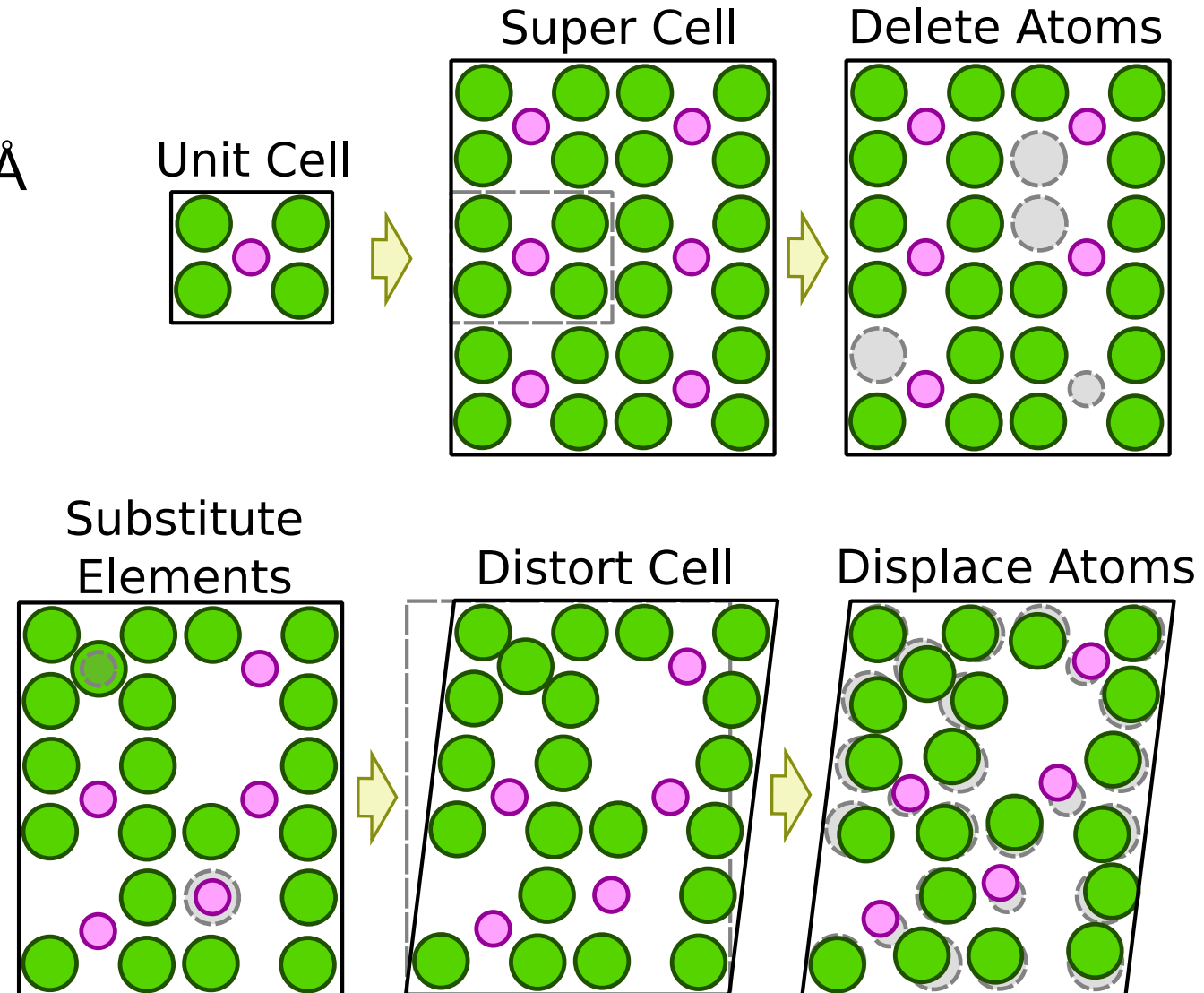
Computational Details

- DFT with VASP:
 - PBE Functional
 - PW cut-off 600 eV
 - 20,000 kpprÅ³ (\approx 27 kpprÅ)
- Structure enumeration with **icet**
- Module implemented ASE (not yet upstream):
 - Arbitrary committees from **calculator** mixing
 - Committees augmented uncertainty bias term
 - Biased contour exploration



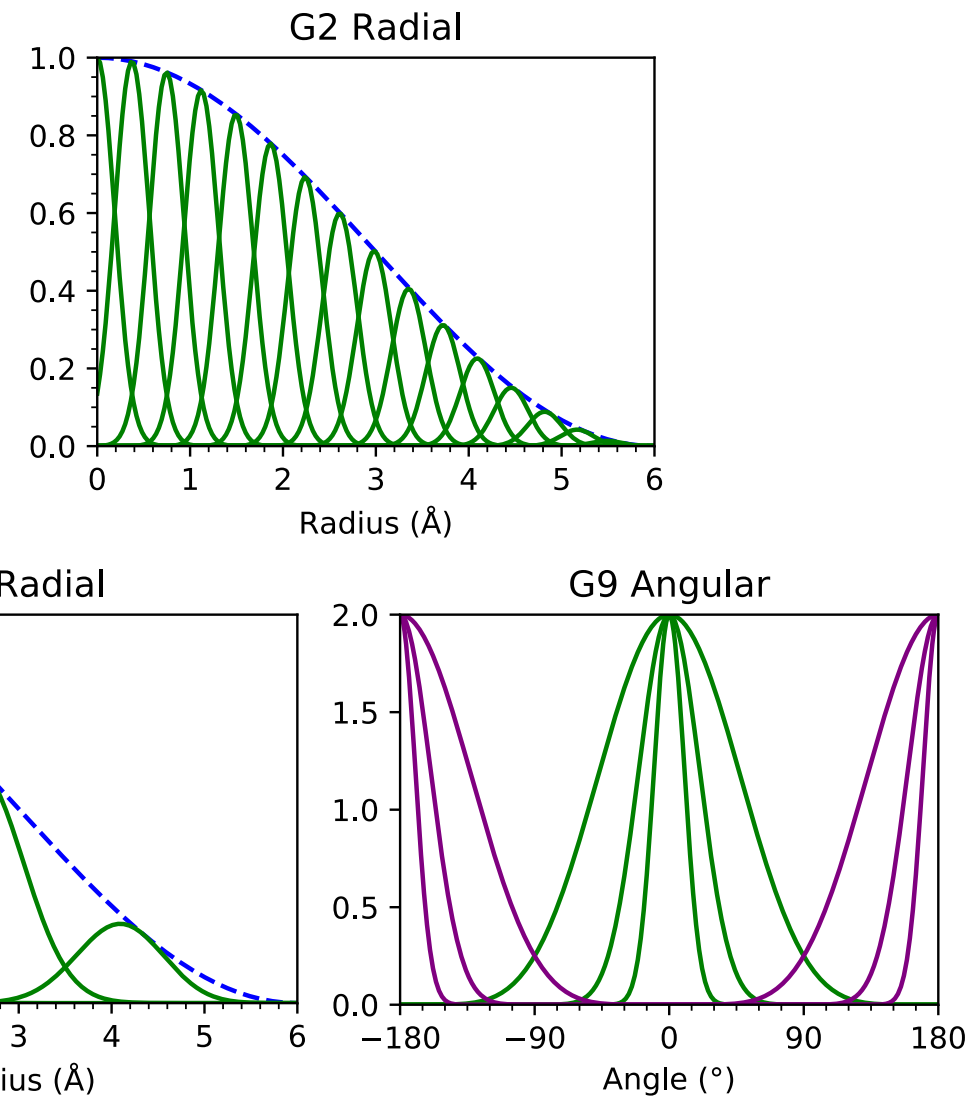
Derived Structure Procedure

- Atom displacements (stdev): $0.4/0.3 \text{ \AA}$ (metals/oxides)
- Volume strain range: -2.5% to +7.5%
- Von Mises strain max: 20%
- Deletion chance: 5%
- Substitution chance = 50%/10% (metals/oxides)



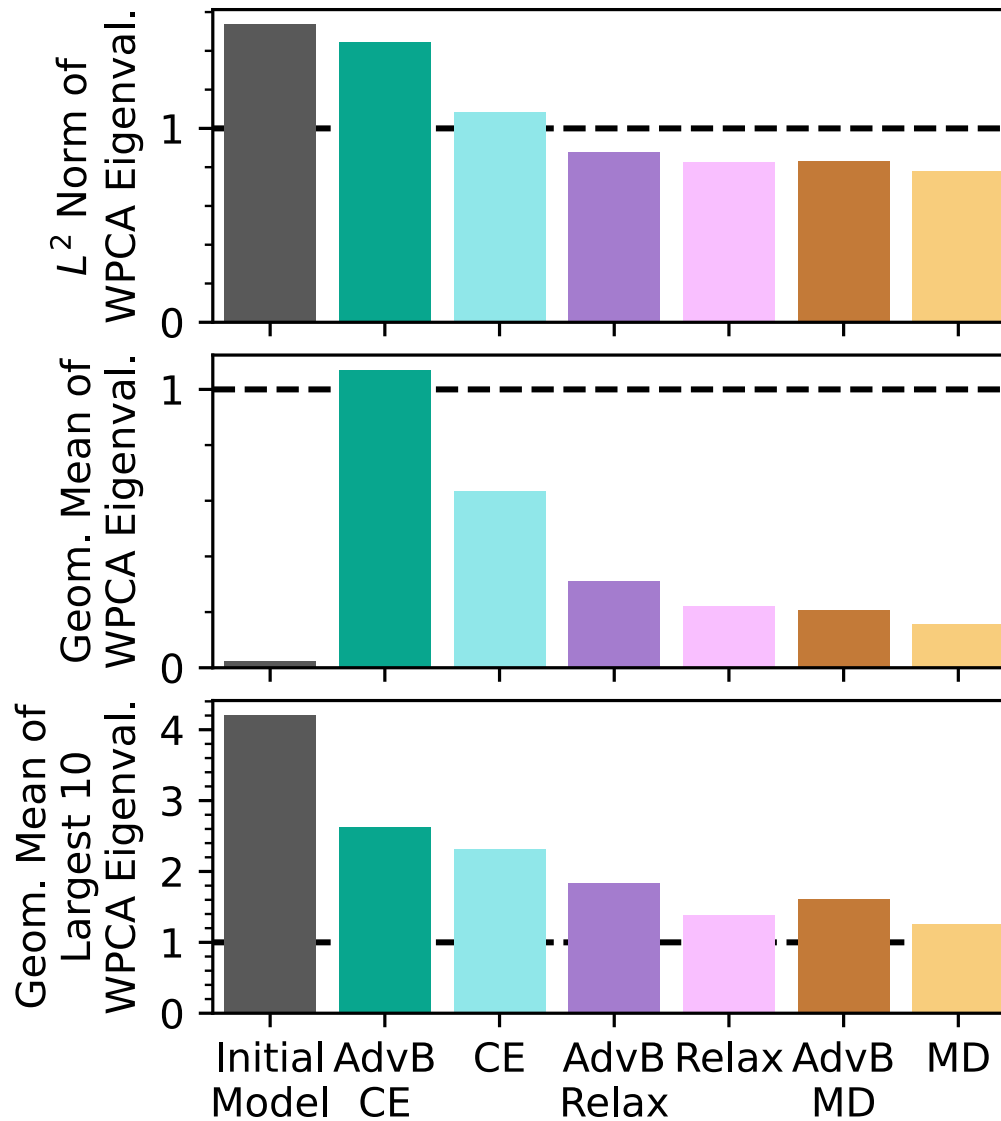
C-MLIP Parameters

- Using $n2p2$
 - (<https://compphysvienna.github.io/n2p2/>)
- **8** MLIPs in committee
 - (10,10) neural net
 - 6 Å radial cut
 - 16 radial Behler-Parrinello G2 per pair
 - ‘wide angle’ Behler-Parrinello G9 per triplet
 - 3 radial x 6 angular = 18
- Training
 - 600 epochs of Kalman filter
 - 0.2 force weight, worst 3% of forces each epoch



Diversity

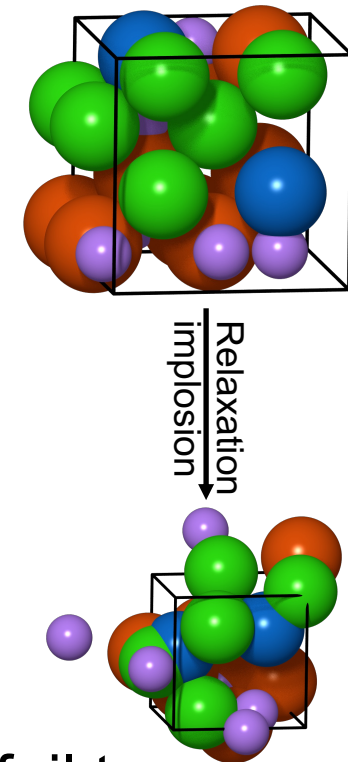
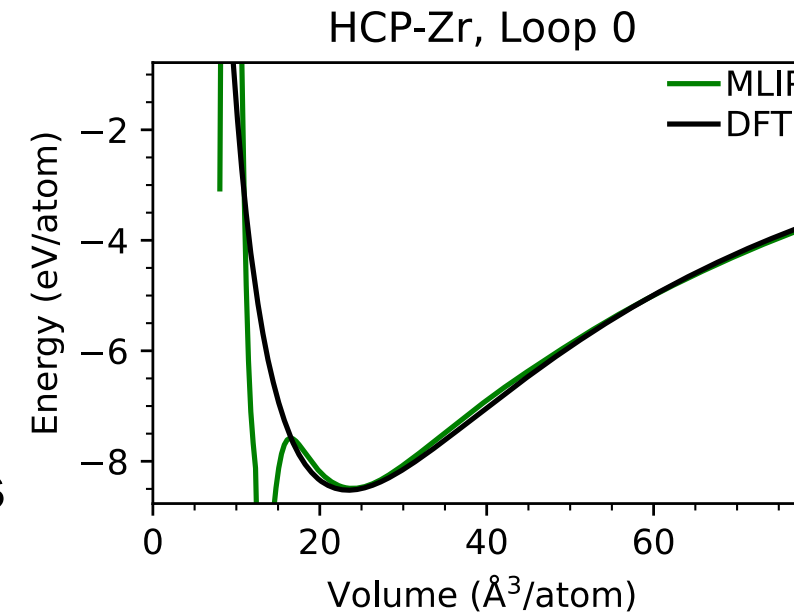
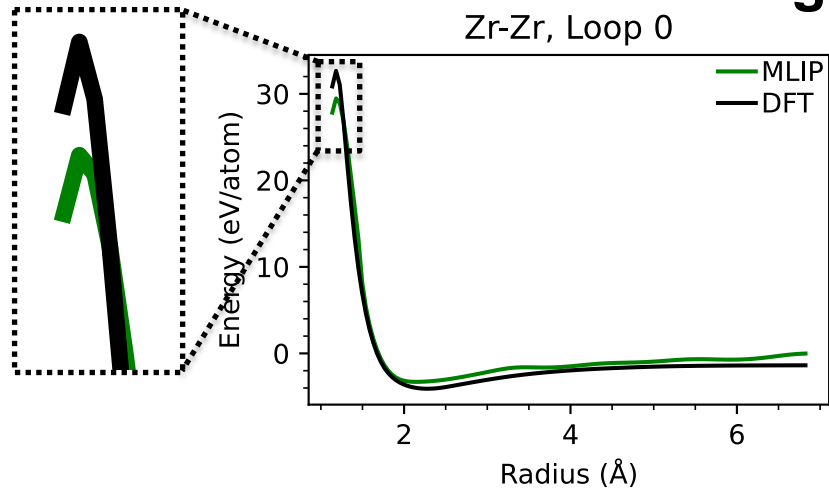
- Structure enumeration produces diverse data even if not informative data



Extra Slides 4

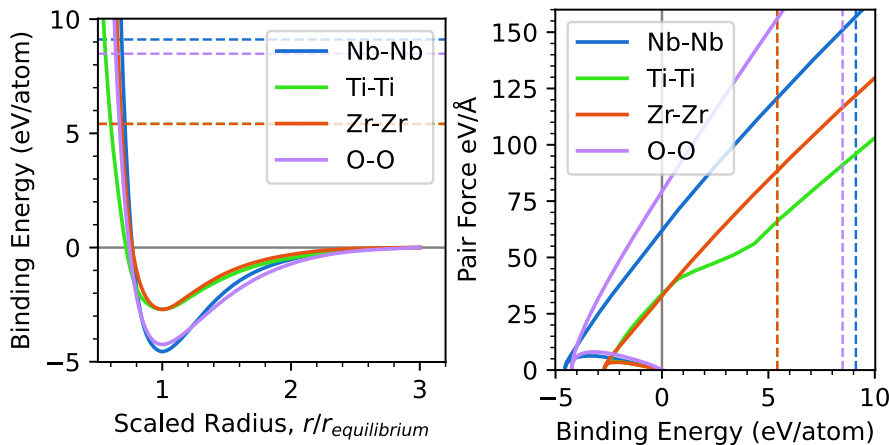
Automating Saddle Searches

A great way to find MLIP instabilities



Uncorrectable pseudopotential instabilities

- Block with by radius & force limits



Correctable instabilities

- Add initial structures that fail to relax to *unrelaxed* training set

Implementation Details



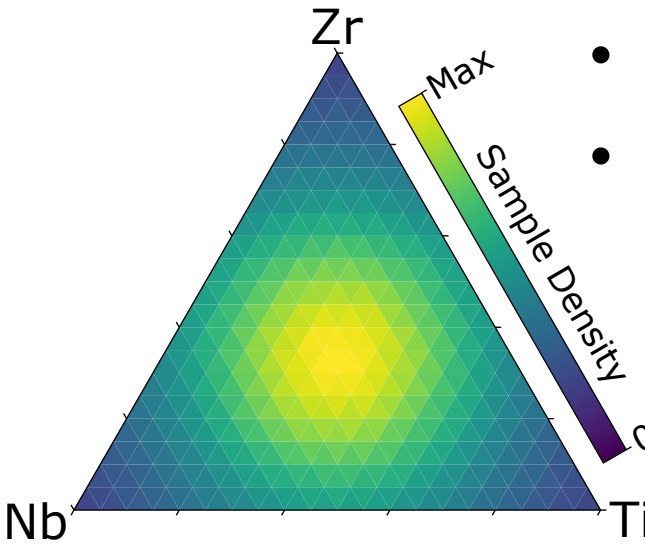
- Random structure generation: icet
- Saddle finding and general automation: ASE
- ACE model for MLIP: Pacemaker
 - $r_{\text{cut}} = 7 \text{ \AA}$
 - Radial functions by body order: <20, 4, 2, 1>
 - Angle function I_{\max} by body order: <0, 5, 2, 1>
- DFT calculations: VASP
 - PBE Functional
 - PW cut-off 600 eV
 - 20,000 kppr \AA^3 (\approx 27 kppr \AA)



pacemaker

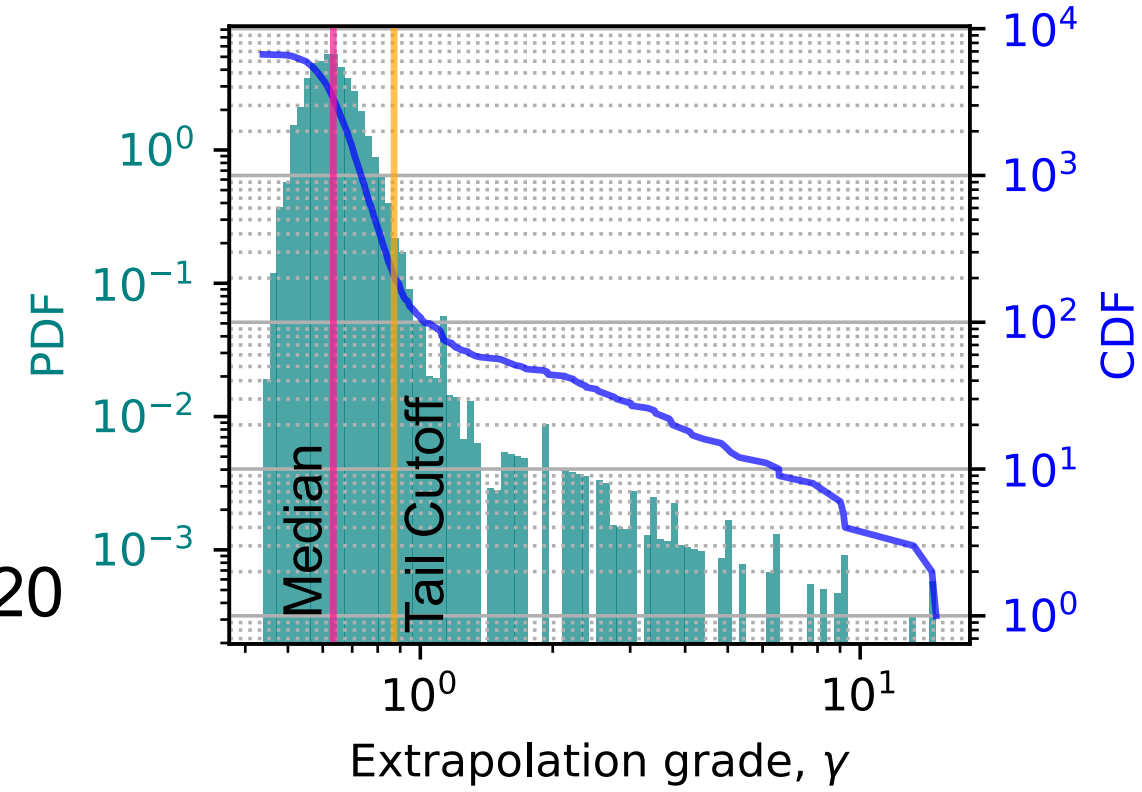


Composition and Active Learning Selection



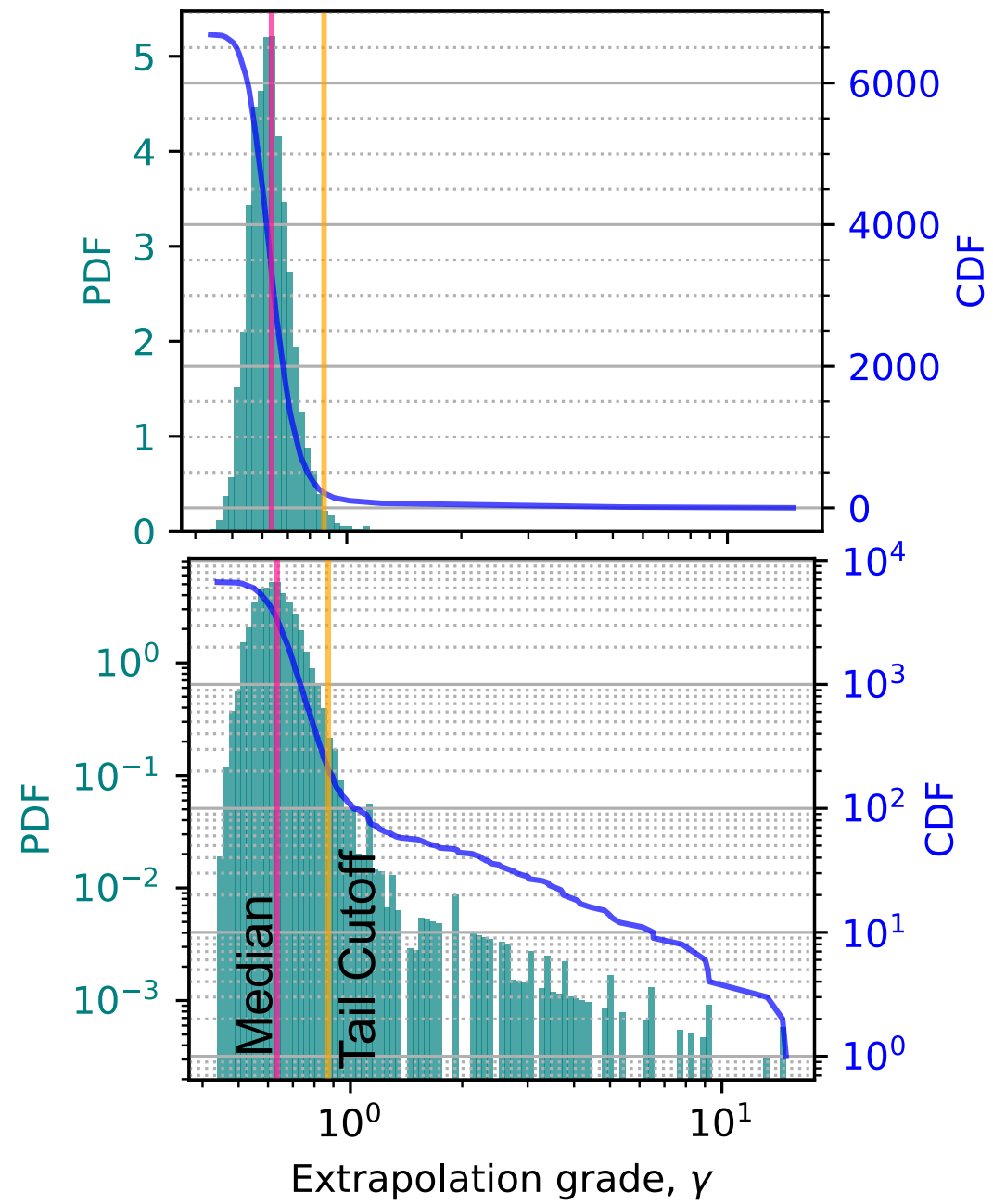
- Sampling biased towards equimolar alloys (~4:1)
- 0-30 at% oxygen interstitials

- Sample structures *until* ~200 in extrapolation grade tail (2-3%)
- Tail selection train/test split: 80/20
 - Challenging test set



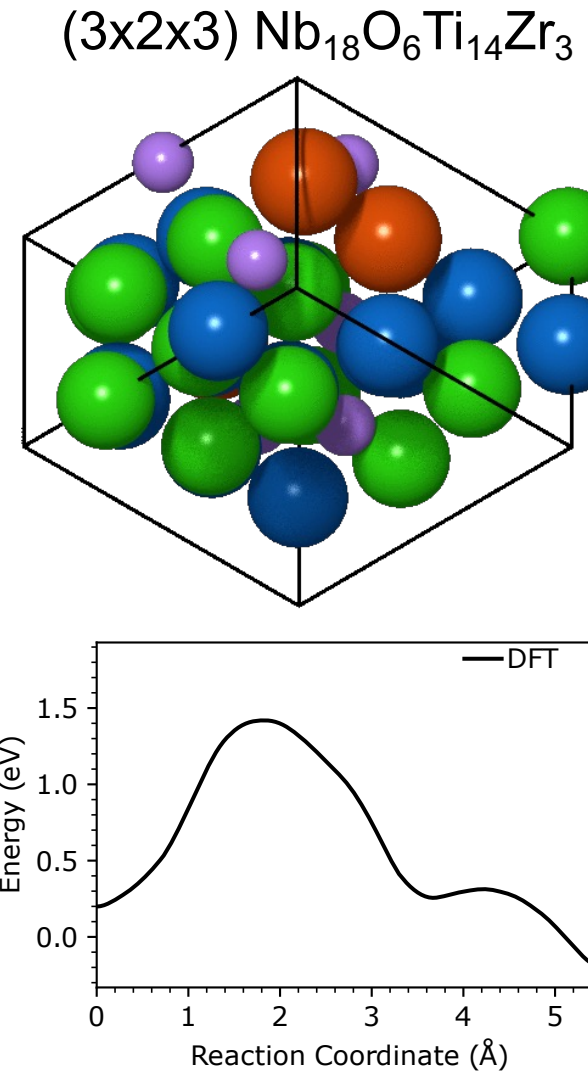
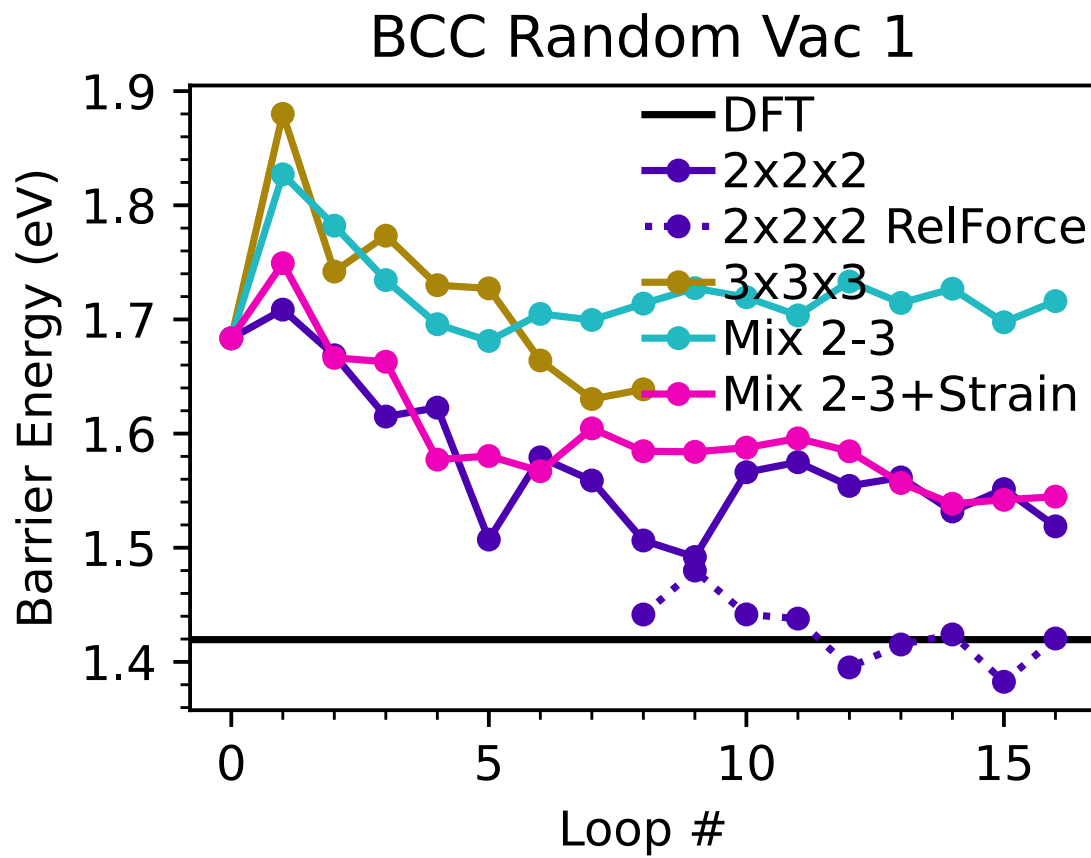
Tail Sampling

- Median is closer to PDF peak than mean
- Gaussian-like in $\ln \gamma$
- Tail cutoff = 1.5x second moment above median of $\ln \gamma$



Random BCC Alloy Diffusion

- Mimics structure of target application



Demonstration

- Oxygen diffusing away a Ti site in BCC Nb
- Oxygen prefers Ti

